https://doi.org/10.1016/j.atmosenv.2019.117068

Evaluation and Comparison of Himawari-8 L2 V1.0, V2.1 and MODIS C6.1 aerosol products over Asia and the Oceania regions

Xingchuan Yang [a, b], Chuanfeng Zhao [a], Nana Luo [f], Wenji Zhao [b],

Wenzhong Shi [e], Xing Yan [a*]

a College of Global Change and Earth System Science, Beijing Normal University, Beijing, China

b College of Resource Environment and Tourism, Capital Normal University, Beijing, China

c State Key Laboratory of Remote Sensing Science, Beijing Normal University, Beijing, China

d Department of Atmospheric and Oceanic Science, and Earth System Science Interdisciplinary Center, University of Maryland, College Park, Maryland, USA

e Department of Land Surveying and Geo-Informatics, The Hong Kong Polytechnic University, Hong Kong, China

f Department of Geography, San Diego State University, 5500 Campanile Dr., San Diego, CA 92182-4493, USA

*Corresponding author:

Xing Yan

GCESS, Beijing Normal University, 19 Xinjiekouwai Street, Haidian, District, Beijing 100875, China.

Email: yanxing@bnu.edu.cn

Abstract

Himawari-8 aerosol products are useful for forecasting weather, environmental monitoring, and climate change research. In 2018, after receiving much attention from researchers, the Himawari-8 Level2 (L2) aerosol retrieval algorithm was updated from Version 1.0 (V1.0) to Version 2.1 (V2.1). Although previous studies have examined the accuracy of Himawari-8 aerosol products, only a few studies have evaluated and compared the V1.0 and V2.1 algorithms or described how the Himawari-8 aerosol products differ from those of MODerate-resolution Imaging Spectrometer (MODIS). In this study, we validated and compared the Himawari-8 L2 V1.0 and V2.1 aerosol products at 500 nm using data from all Asian Aerosol Robotic Network (AERONET) sites for the period from 2016 to 2017. Furthermore, a comprehensive comparison between the Himawari-8 L2 V2.1 and MODIS C6.1 AOD (Terra and Aqua) products was conducted. The V1.0 and V2.1 AOD agreed well with AERONET AOD (R: 0.67-0.72) with 44.65% and 49.38% of retrievals fell within the EE, respectively. Meanwhile, V1.0 and V2.1 AOD bias increased with the AOD magnitude, but V1.0 AOD tended to underestimate the AOD. The underestimation has now improved in the V2.1 AOD products. Both V1.0 and V2.1 AOD performed better over forests and grasslands than croplands, as well as urban and barren lands and had the best performance in summer, while the worst in spring. Overall, the V2.1 AOD outperformed in term of retrievals falling within the EE compared to V1.0 AOD, but it still has large estimation uncertainties in high aerosol loadings areas and sparsely vegetated areas, which indicating the aerosol algorithm needed to improve in the future. Furthermore, the data quality of V2.1 AE/FMF products significantly improved compared to that of V1.0. Compared to the MODIS C6.1 AOD products, Himawari-8 L2 V2.1 AOD accuracy is slightly lower but demonstrates a similar spatial distribution.

1. Introduction

Atmospheric aerosols are suspensions of liquid and solid particles in the atmosphere that are generated from a wide range of natural and anthropogenic sources. Atmospheric aerosols significantly affect the global climate system directly by scattering and absorbing incoming solar radiation and indirectly by altering cloud formation and their properties (IPCC, 2013; Levy et al., 2013; Li et al., 2016). Moreover, high concentrations of aerosol particles can cause serious environmental problems and threaten public healthy (Butt et al., 2016). Therefore, obtaining accurate aerosol data is vital to climate, atmospheric, and environmental studies.

Aerosol optical properties can be monitored using ground-based measurements and satellite-based observations. Ground-based measurement networks, such as Aerosol Robotic Network (AERONET), provide accurate multispectral data of aerosol optical properties, including aerosol optical depth (AOD), Ångström exponent (AE), and fine-mode fraction (FMF), with a high temporal resolution (HOLBEN et al., 1998). However, AERONET sites are limited in number and are unevenly distributed across the globe, making it impossible to retrieve information on aerosol properties worldwide. Satellite-based measurements are an increasingly popular method of obtaining aerosol data as it provides large-scale aerosol spatial data that is vital to climate and environmental research (Chu et al., 2003; Paasonen et al., 2013; Remer et al., 2008; Saide et al., 2015; Yan et al., 2017). With the rapid development in satellite observation technologies, a series of sensors with high spectral, spatial, and temporal resolutions, as well as multi-angle capabilities, have been launched. These include the MODerate Resolution Imaging Spectroradiometer (MODIS), Multi-angle Imaging SpectroRadiometer (MISR), and Visible Infrared Imaging Radiometer Suite (VIIRS). Many sophisticated algorithms for retrieval of information on the AOD have been developed, such as the Dark Target (DT)(Kaufman et al., 1997; Levy et al., 2013), Deep Blue (DB)(Hsu et al., 2013; Hsu et al., 2004), and MISR algorithm (Diner et al., 2005).

The MODIS sensor has proven its superiority by continually providing aerosol products over land and ocean with excellent spatiotemporal resolution. Many studies have evaluated the retrieval accuracy of aerosol products from MODIS(Bilal et al., 2017;Gupta et al., 2018; Levy et al., 2010; Sayer et al., 2013; Sayer et al., 2014; Sayer et al., 2015). Evaluation studies on AOD products retrieved using the recently released MODIS Collection 6.1 (C6.1) indicated that the latest C6.1 measurements have the high agreement with those from the AERONET. However, MODIS is mounted on a polar-orbiting satellite, which makes it difficult to capture dynamic aerosol characteristics. In contrast, geostationary earth orbits (GEO) satellites hover over a single location with respect to the Earth, providing constant and dynamic monitoring of the Earth with high temporal resolution (Yan et al., 2018). Himawari-8 is the next-generation of geostationary meteorological satellites that were launched by the Japan Meteorological Administration (JMA) on October 7, 2014. Himawari-8 carries the Advanced Himawari Imager (AHI) onboard and has 16 spectral channels (3 visible, 3 near-infrared and 10 infrared), with visible channel spatial resolutions of 0.5-1 km and an infrared channel resolution of 2 km (Bessho et al., 2016). Himawari-8 can provide diurnal aerosol properties every 10 minutes for the Asia-Pacific region and every 2.5 minutes for Japan Area and Target Area.

Japan Aerospace Exploration Agency (JAXA) released Himawari-8 L2 V1.0 aerosol products in December 2016, followed by the updated V2.1 aerosol products in August 2018. Himawari-8 aerosol products provide information critical to monitor regional air pollution (Wang et al., 2017; Zang et al., 2018), dust (Sekiyama et al., 2016), and wild fires (Wickramasinghe et al., 2016). Thus, the evaluation of retrieval accuracy and uncertainties in Himawari-8 aerosol products is very important. However, to date, there are still a few studies that address this issue. For example, Wang et al. (2017) evaluated the accuracy of Himawari-8 L3 AOD retrievals in Beijing and found that the Himawari-8 L3 AOD retrievals exhibited high correlations (R^2: 0.74–0.81) and low uncertainty (0.18–0.22) with 54–59% of the retrievals falling within the expected error (EE). Zhang et al. (2018) reported that Himawari-8 L2 AOD in China had a high correlation (R^2 = 0.67) with AERONET measurements, and 55% of the AOD retrievals fell within the EE; according to the authors, the accuracy of L2 AOD was observed to be highly dependent on seasons and surface land cover types. Yang et al. (2018) found out that Himawari-8 L3 AOD measurements underestimated the actual AOD and performed slightly poorer than MODIS DB and DT in China. However, these studies were mainly focused on particular regions or single countries with insufficient AERONET sites included in the data. Therefore, it is difficult to gauge the retrieval accuracy of Himawari-8 aerosol products in Asia and the Oceania region. Further in-depth research is needed on the limitations of retrieval algorithms and factors influencing their retrieval accuracy. In this study, we have comprehensively evaluated the Himawari-8 L2 V1.0 and V2.1 aerosol products from 2016 to 2017, allowing a more detailed comparison of the retrieval accuracy of Himawari-8 and MODIS AOD products over Asia.

2. Data and methods

2.1. Study area

The Himawari-8 is located at the equator at 140°E longitude; it has an observation range of 80ºE ~ 160ºW and 60ºS ~ 60ºN, covering East Asia and Southeast Asia, the western Pacific Ocean, Oceania. Fig. 1 shows the geographical distribution of the selected 58 AERONET sites in Himawari-8 observation domain. Table S1 provides the detailed information about the AERONET sites. These stations are located in areas that are influenced by different aerosol types. The source of aerosols in mainland Asia and the surrounding oceanic regions are a mix of various types, including anthropogenic aerosols from industry, automobiles or other human activities in urban areas, crop residue burning, as well as natural aerosol from mineral dust (Mehta et al., 2016). In the past few decades, with the rapid development of economies and populations in developing countries, such as China and India, the amount of anthropogenic aerosols released into the atmosphere has rapidly increased (Zhang et al., 2012). The sources of aerosols in Australia and the surrounding oceanic regions are mostly based on mineral dust from their arid interiors and smoke from biomass burning in the tropical north (Schepanski, 2018).

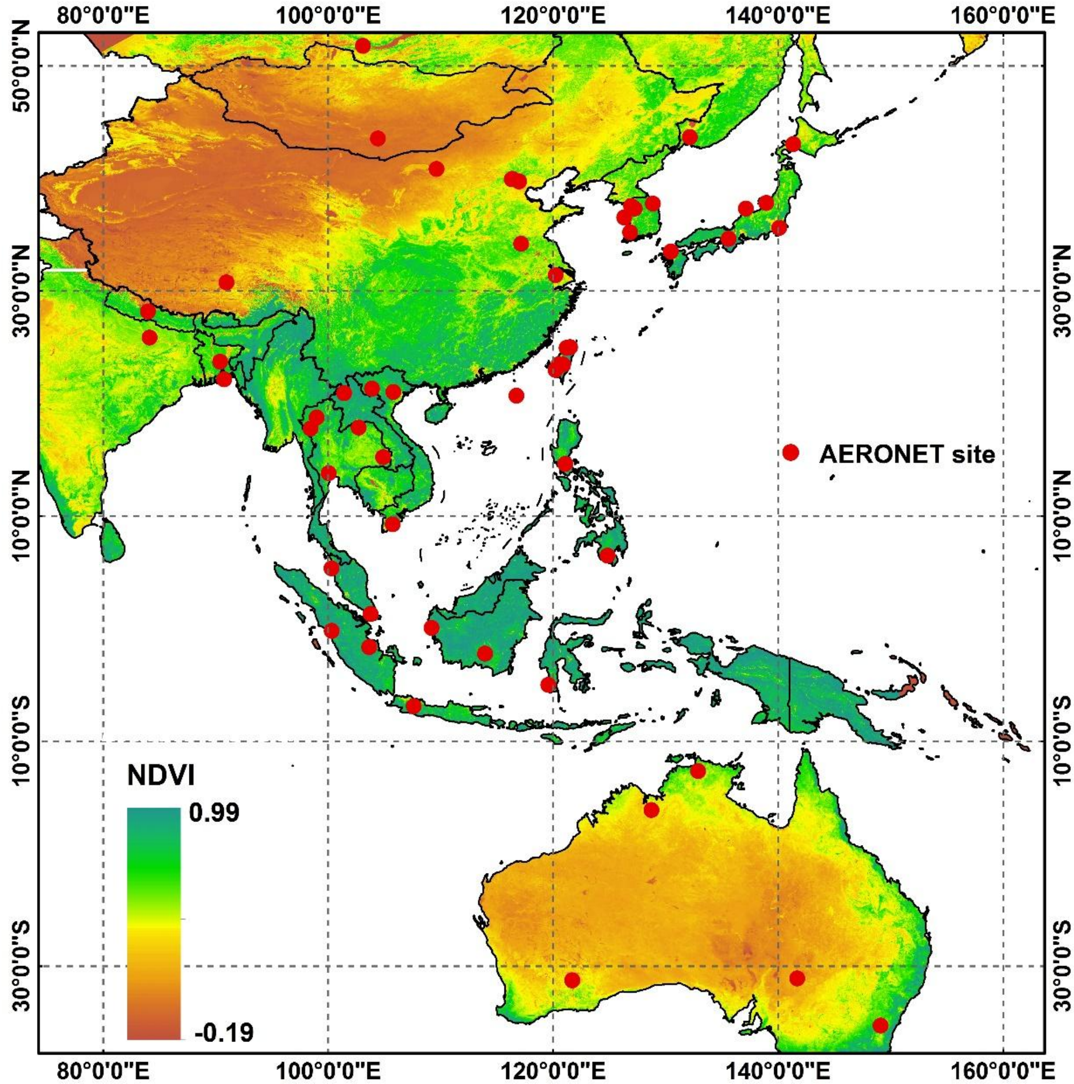

Fig. 1. Study area and locations of AERONET sites (red dots). The background image depicts 2-year (2016-2017) annual average MODIS NDVI.

2.2 Data

2.2.1 Himawari-8 aerosol products

Himawari-8 L2 aerosol products include aerosol optical depth at 500 nm, Ångström exponent (AE) and optical depth ratio (FMF) with the temporal and spatial resolutions of 10 min and 5 km, respectively. The Himawari-8 L2 AOD, AE, and FMF products (QA=ALL and QA=Very good) were obtained from JAXA (http://www.eorc.jaxa.jp/ptree) from January 2016 to December 2017 over the study area (from 00:00 to 09:50 Coordinated Universal Time, UTC) (Table 1).

There are three algorithms used in the Himawari-8 L2 aerosol product, including V1.0, V2.0 and V2.1. For aerosol model of V1.0 algorithm, aerosol type is assumed to be Asian dust and aerosol particles are assumed to be spheroidal and randomly oriented (Mano et al. 2009). For surface reflectance, land surface reflectance is simulated using the near-infrared band (2300 nm), while the ocean surface is simulated using multiple facets whose slopes vary with wind speed over the ocean (Cox and Munk 1954). As compared to the V1.0 algorithm, the V2.1 algorithm has major improvements in aerosol models, surface reflectance estimation, and maximum AOD output. For the aerosol model in the V2.1 algorithm, the fine aerosol model parameters were set according to the average properties of fine models numbered 1-6 as defined by Omar et al. (2005), while the pure marine aerosol model parameters were set according to the model defined by Sayer et al. (2012). Both models were assumed to be spherical. The dust aerosol model parameters were set according to the coarse model by Omar et al. (2005) and was assumed to be a non-spherical. For the surface reflectance estimation, the V2.1 algorithm was used with the Rayleigh scattering-corrected reflectance for each band that had the second lowest reflectance at 470 nm in one month as the surface reflectance. When the surface reflectance value at 470 nm was higher than at 640 nm, it was estimated using the improved Kaufman method (Fukuda et al., 2013). In addition, the V2.1 algorithm improved the implementation of the iteration of optical estimation and expanded the AOD range from 2.0 to 5.0.

2.2.2 MODIS AOD products

The MODIS instrument onboard the Terra and Aqua satellites of the Earth Observing System (EOS) is operated by the National Aeronautics and Space Administration (NASA) (Salomonson et al., 1989). The Terra satellite passes the equator at about 02:30 (UTC), while Aqua passes the equator at about 05:30 (UTC). The MODIS AOD products provide a consistent record of global aerosol information. In this study, the DB 10 km AOD (Scientific Data Set (SDS): Deep Blue Aerosol Optical Depth 550 Land Best Estimate) (QA$\geqslant$2 for land), DT 10 km AOD (SDS:

Optical Depth Land And Ocean) (QA=3), and DT 3 km AOD (SDS: Optical Depth Land And Ocean) (QA=3) of MODIS Collection 6.1 Terra and Aqua were used to compare the accuracy and regional distribution of Himawari-8 AOD products over Asia (Table 1). These products can be downloaded from the NASA DACC website (https://ladsweb.modaps.eosdis.nasa.gov).

2.2.3 AERONET data

AERONET provides globally distributed observations of spectral columnar AOD with low uncertainty (0.01-0.02) and high temporal resolution (every 15 min) and is commonly used to evaluate satellite AOD products (Eck et al., 1999). In this study, AERONET version 2 data were collected from 58 AERONET sites over the study area for validation purposes. Because the AERONET quality assurance level of 2.0 was not achievable during all periods, level 2.0 spectral deconvolution algorithm (SDA) data were used, when available. Level 1.5 SDA data were used at all other times. More detailed information regarding the AERONET data is given in Supplementary Table S1.

2.2.4 Vegetation indices, DEM, and land cover data

Surface type is the most important factor affecting the satellite-based aerosol retrieval accuracy. In this study, the MODIS Land Cover Type product (MCD12Q1), the MODIS vegetation index product (MOD13A3), and the Shuttle Radar Topography Mission (SRTM) 90-m digital elevation model (DEM) data were used to explore their relationship with errors observed in the Himawari-8 AOD products. The MCD12Q1 provided information on the annual global land cover based on five global land cover classification systems (Friedl et al., 2010) (https://e4ftl01.cr.usgs.gov/MOTA/MCD12Q1.006/), and the MOD13A3 provided global vegetation index data with 1-km resolution (https://e4ftl01.cr.usgs.gov/MOLT/MOD13A3.006/). The SRTM 90-m resolution DEM provides digital elevation data for more than 80% of the world between 60°N and 56°S (http://srtm.csi.cgiar.org/ Index.asp).

Table 1. Summary of datasets used in this study

Instrument/Product	SDS name	Resolution	Coverage
Himawari-8 L2 Version1.0 Himawari-8 L2 Version2.1	Aerosol optical thickness; Ångström exponent; Optical Depth Ratio (FMF)	10 min, 5 km; 00:00-09:50 (UTC)	80ºE ~ 160ºW 60ºS ~ 60ºN
MOD04_L2 MYD04_L2	Deep_Blue_Aerosol_Optical_Depth_550_Land_Best_Estimate Optical_Depth_Land_And_Ocean	Daily, 10 km; 02:30/05:30 (UTC)	Global
MOD04_3K MYD04_3K	Optical_Depth_Land_And_Ocean	Daily, 3 km; 02:30/05:30 (UTC)	
MOD13A3	1 km monthly NDVI	Monthly, 1 km	
MCD12Q1	Land Cover Type Yearly L3 Global 500 m SIN Grid	Year, 0.5 km	
AERONET	Aerosol Optical Depth (V2) ; AE (α) ; FMF	15 min, Site	
SRTM	90 m Digital Elevation Data	Year, 90 m	

2.3 Data processing and analytical methods

To match satellite data with AERONET observations, wavelength interpolation and spatial-temporal matching processing are required. Himawari-8 AOD products were directly compared with the AERONET AOD data at 500 nm. MODIS AOD retrievals at 550 nm from both Terra and Aqua satellites were evaluated in this study. Since AERONET AOD products do not include the 550-nm channel, to compare with MODIS AOD retrievals, first the AE (α) was calculated based on AOD wavelengths of 440 and 675 nm (Eq. (1)). Moving on, AERONET AOD was obtained at 550 nm by interpolating the AERONET data with AE (Eq. (2)).

$$\alpha = -\frac{\log\frac{\tau_1}{\tau_2}}{\log\frac{\lambda_1}{\lambda_2}} \qquad (1)$$

Where λ_1 and λ_2 are different wavelengths (440 and 675 nm), and τ_1 and τ_2 are the AOD at λ_1 and λ_2.

$$\tau_\lambda = \beta\lambda^{-\alpha} \qquad (2)$$

Where λ is the wavelength, τ_λ represents the AOD at wavelength λ, α is the wavelength exponent; and β is turbidity coefficient.

Previous validation studies of satellite AOD products generally consider spatial window sizes of 3 × 3 and 5 × 5 centered at each AERONET site(Gupta et al., 2018; Nichol & Bilal, 2016; Xiao et al., 2015), which can increase the number of matched AODs for those sites without long-term measurements. However, the large window size may introduce unexpected errors due to topographic or aerosol type heterogeneity (Yong et al., 2011). In this study, to focus on the fine-scale AOD, the single satellite pixel closest to the AERONET coordinates was used; this validation method is the same as that used for the MAIAC AOD validation described by Emili et al. (2011). Then AERONET AOD averaged within ±30 min of the MODIS overpass were extracted for matching MODIS C6.1 AOD products and its averaged values for ±5 min of the Himawari-8 overpass were extracted for matching Himawari-8 L2 AOD products.

To quantitatively evaluate the accuracy of different AOD products, several statistical techniques were used. Pearson correlation coefficient was used to analyze the correlation between retrievals and measured values. The root mean squared error (RMSE, Eq. (3)), mean absolute error (MAE, Eq. (4)), relative mean bias (RMB, Eq. (5)), and Mean bias (Eq. (6)) (Mhawish et al., 2017) were used to evaluate the uncertainty in aerosol retrievals. Furthermore, the expected error (EE, Eq. (7)) have been used to evaluate the retrieval accuracy (Chu et al., 2002).

$$\mathrm{RMSE} = \sqrt{\frac{1}{n}\sum_{i=1}^{n}\left(AOD_{(Satellite)i} - AOD_{(AERONET)i}\right)^2} \quad (3)$$

$$\mathrm{MAE} = \frac{1}{n}\sum_{i=1}^{n}\left|AOD_{(Satellite)i} - AOD_{(AERONET)i}\right| \quad (4)$$

$$\mathrm{RMB} = \frac{1}{n}\sum_{i=1}^{n}\left|AOD_{(Satellite)i}/AOD_{(AERONET)i}\right| \quad (5)$$

$$\text{Mean bias} = \frac{1}{n}\sum_{i=1}^{n}\left(AOD_{(Satellite)i} - AOD_{(AERONET)i}\right) \quad (6)$$

$$\mathrm{EE} = \pm(0.05 + 0.15AOD_{AERONET}) \quad (7)$$

3. Results

3.1 Evaluation of Himawari-8 L2 AOD retrieval accuracy against AERONET

3.1.1 Overall accuracy of V1.0 and V2.1 AOD products

To evaluate the performance of the Himawari-8 L2 AOD retrievals, a total of

76,362 pairs of Himawari-8 and AERONET AOD retrievals at 500 nm were obtained from 58 stations from 2016 to 2017. Both V1.0 and V2.1 AOD represented high agreement with AERONET AOD (R: 0.67-0.72). There were 44.65% of retrievals from V1.0 AOD that fell within the EE, and 44.65% (11.70%) were underestimated (overestimated) (Fig. 2(a)). For V2.1 AOD products, 49.38% of the measurements were within the envelopes of EE and 24.17% (26.45%) were underestimated (overestimated) (Fig. 2(b)). The V1.0 AOD appeared to have comparatively lower RMSE (0.26) and MAE (0.17), compared to the V2.1 AOD (R: 0.67, RMSE: 0.37, MAE: 0.19). Fig. 3(a) and (b) illustrate the difference between V1.0 AOD and V2.1 AOD against AERONET AOD, respectively. V1.0 and V2.1 AOD showed relatively small bias, when the AOD was lower than 0.3. When the AOD was greater than 0.4, the bias increased with the AOD magnitude. For V1.0 AOD, the AOD showed a negative bias mostly at low and high AOD values, which indicated that V1.0 AOD retrievals underestimated AOD. The V2.1 AOD had a smaller mean bias (-0.08), which showed about zero mean bias at most AOD values (AOD<1.4) as compared to that of V1.0 AOD. Furthermore, according to the standard deviation in AOD bins, the standard deviation for V2.1 AOD increased with the AOD magnitude, while the standard deviation for V1.0 varied less.

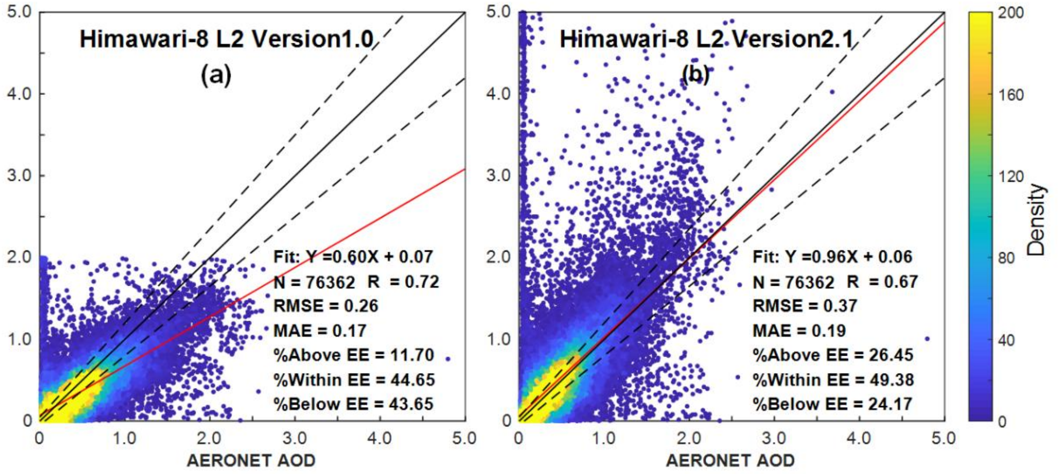

Fig. 2. Evaluation of Himawari-8 L2 V1.0 (a) and V2.1 (b) AOD retrievals at 500 nm against AERONET AOD measurements at 500 nm for all stations from 2016 to 2017. Data are sorted into

pairs (AERONET, Himawari-8) of AOD retrievals at 0.05 intervals of AOD. That color represents the number of cases (color bar) with the value of a given pair, i.e., frequency. Linear regression is shown as a solid red line and all the linear relationships are statistically significant at α=0.01. The dashed lines are the envelopes of the expected error, while the black solid line is the 1:1 line.

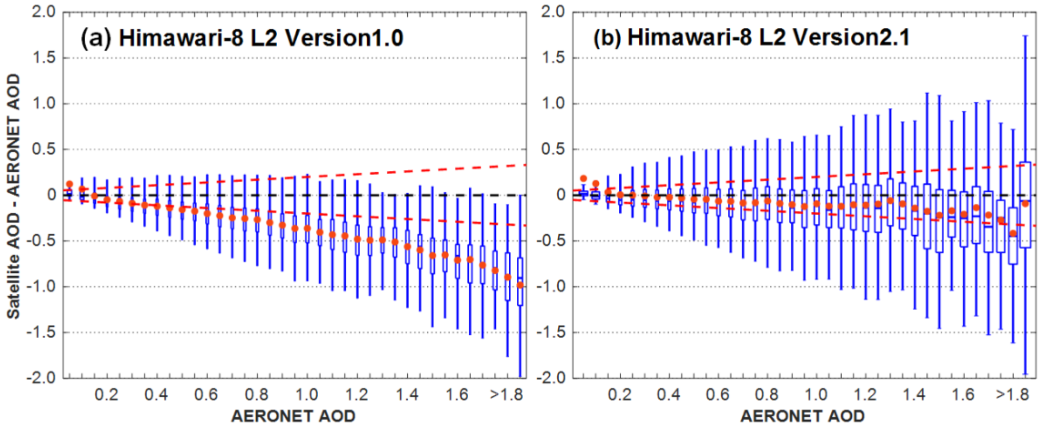

Fig. 3. Box plots of Himawari-8 L2 V1.0 (a) and V2.1 AOD (b) errors (satellite - AERONET) at 500 nm versus AERONET AOD. Data are sorted by AERONET AOD at 0.05 intervals of AOD. The one-one line (zero error) is shown as a black dashed line, and the envelopes of the expected error are shown as red dashed lines. For each box-whisker plot, the width is the standard deviation (α) of the satellite AOD measurement; height is the interquartile range of the AOD error; the middle line and the red dot are the median and mean bias, respectively.

Seasonal variations in surface reflectance can affect the quality of aerosol retrievals (Mhawish et al., 2017). Therefore, we evaluated the performance of Himawari-8 L2 AOD retrievals in different seasons (Table 2). The number of collocation was observed to vary within seasons with spring having the highest collocation (N: 31201), followed by winter (N: 22618) and summer (N: 12620). Fall appeared to have the lowest collocation (N: 9923). For the V1.0 and V2.1 AOD products, a better performance was recorded in summer and fall than that in spring and winter. There was more than 48% of V2.1 AOD within the EE envelops for these two seasons, while more than 42% exhibited this trend for V1.0 AOD. The V1.0 and V2.1 AOD products had a better agreement (R:0.79-0.84) with AERONET AOD with comparatively lower RMSE (0.22-0.27) and MAE (0.14-0.16) in summer and fall, relative to that in spring and winter (R: 0.55-0.68, RMSE: 0.30-0.44, MAE:

0.20-0.27). The result showed that the Himawari-8 L2 AOD retrieval algorithm performs the best in summer and performs the worst in spring. For the four seasons, as compared with the V1.0 AOD, the V2.1 AOD had more retrievals that fell within the EE, but it had higher RMSE and MAE. Additionally, the V2.1 AOD overestimated AOD in all seasons (RMB: 1.03-1.73). The V1.0 AOD underestimated AOD in spring, summer, and fall (RMB: 0.84-0.92), while overestimated AOD in winter (RMB: 1.73).

Table 2. Seasonal summary of error statistics for Himawari-8 L2 V1.0 and V2.1 retrievals against AERONET observations. "MAM," "JJA," "SON" and "DJF" are spring, summer, fall, and winter, respectively, in the Northern hemisphere.

Season	N	RMSE		MAE		RMB		R		(%)Within EE	
		V1.0	V2.1	V1.0	V2.1	V1.0	V2.1	V1.0	V2.1	V1.0	V2.1
MAM	31201	0.37	0.39	0.27	0.23	0.92	1.33	0.68	0.65	27.85	42.39
JJA	12620	0.24	0.27	0.15	0.14	0.87	1.23	0.81	0.79	42.20	55.79
SON	9923	0.22	0.26	0.15	0.16	0.84	1.03	0.84	0.79	44.96	48.82
DJF	22618	0.30	0.44	0.20	0.20	1.28	1.73	0.65	0.55	38.65	47.53

To obtain an overall view of the difference among the Himawari-8 V1.0, V2.1 AOD and AERONET AOD in terms of daily and sub-hourly mean AOD, we generated the time series of this parameter as shown in Figure 4 and Figure 5. Based on the Himawari-8-AERONET matchup data set, the V1.0, V2.1 and AERONET AOD were calculated by averaging all AOD values at each observation time. As illustrated in Figure 4, it was easy to see that the variation of V1.0 and V2.1 AOD dataset were consistent with the ground-based observations ($R \geqslant 0.80$). Both V1.0 and V2.1 AOD products reflected the sub-hourly variability of AOD with higher AOD during 03:00-04:20 (UTC) and lower AOD during 08:50-09:50 (UTC) (Fig.5). However, the V1.0 AOD tended to underestimate AOD at all observation time, whereas the V2.1 AOD product provided relatively high-quality retrievals consistently throughout the day except that it inclined to slightly overestimate AOD during 00:00-00:40 and 05:00-07:20 (UTC) and underestimate AOD during 01:00-04:00 and 08:20-09:50 (UTC).

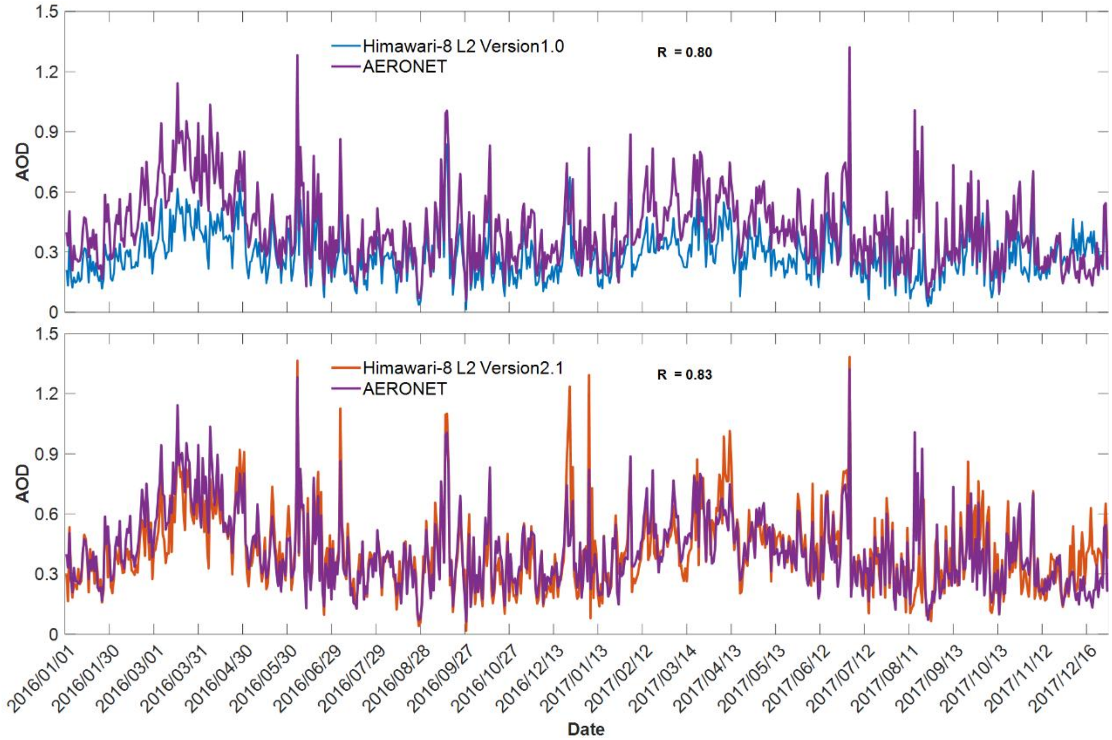

Fig. 4. Time series of daily AOD measurement between Himawari-8 and AERONET.

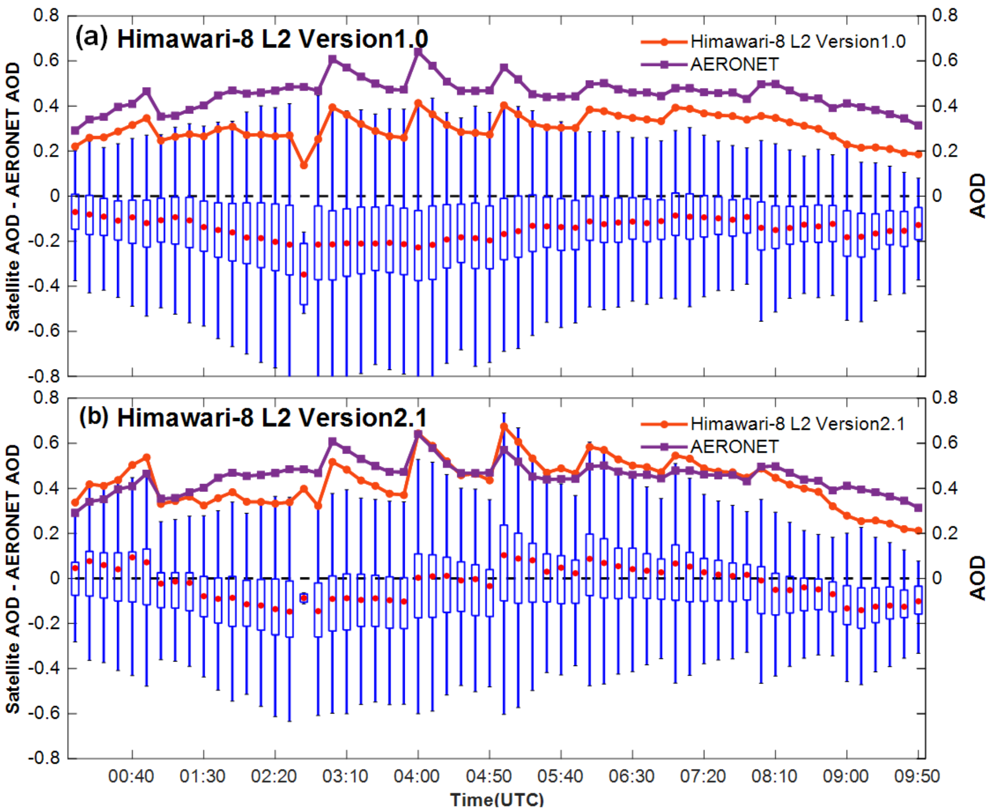

Fig. 5. Box plots of the differences of 10-minute intervals AODs between Himawari-8 and AERONET. For each box-whisker plot, the height is the interquartile range of the AOD error; the red dot is the mean bias.

3.1.2 Site-scale evaluation of V1.0 and V2.1 AOD products

The results of evaluations varied widely with the change of the aerosol model, surface reflectance, and diverse land cover types among all the sites. Therefore, a detailed evaluation of Himawari-8 L2 V1.0 and V2.1 AOD products for site-scale from 2016 to 2017 was conducted in this study (Fig.6). Table S2 presents the corresponding validation statistics. There were 21% and 36% of the sites that had more than 50% of the retrievals falling within the EE for V1.0 and V2.1 AOD, indicating that the V2.1 algorithm is relatively reliable (Fig. 6(a) and (b)). As compared to the V1.0 AOD, the fraction within the EE of V2.1 AOD increased in 47 of the 58 sites. However, for V2.1 AOD, some individual sites located in China (e.g., Dongsha_Island, Lulin, and NAM_CO), Japan (e.g., Osaka and Hokkaido_university), and Australia (e.g., Canberra and Lake_Argyle) had lower numbers of points falling within the EE than that for V1.0 AOD (Fig.6(c)). For V1.0 AOD, approximately 78% of sites had an RMSE of less than 0.3, while V2.1 AOD had only 60% of the sites with an RMSE of less than 0.3 (Fig.6(d) and (e)). Moreover, the RMSE of the V2.1 algorithm at 36 sites was greater than that of the V1.0 algorithm. Small RMSE values of <0.2 were mainly observed in Japan, Korea, and Russia, while large RMSE values of >0.3 were mainly observed in China, Thailand, and Vietnam (Fig. 6(f)). From Fig. 6(g), we can see that the V1.0 algorithm underestimated AOD with more than 77% of the sites having RMB less than 1, especially in Southeast Asia and South Asia. By contrast, the V2.1 algorithm showed better performances in terms of RMB with 44% of the sites having RMB less than 1 (Fig.6(h) and 6 (i)).

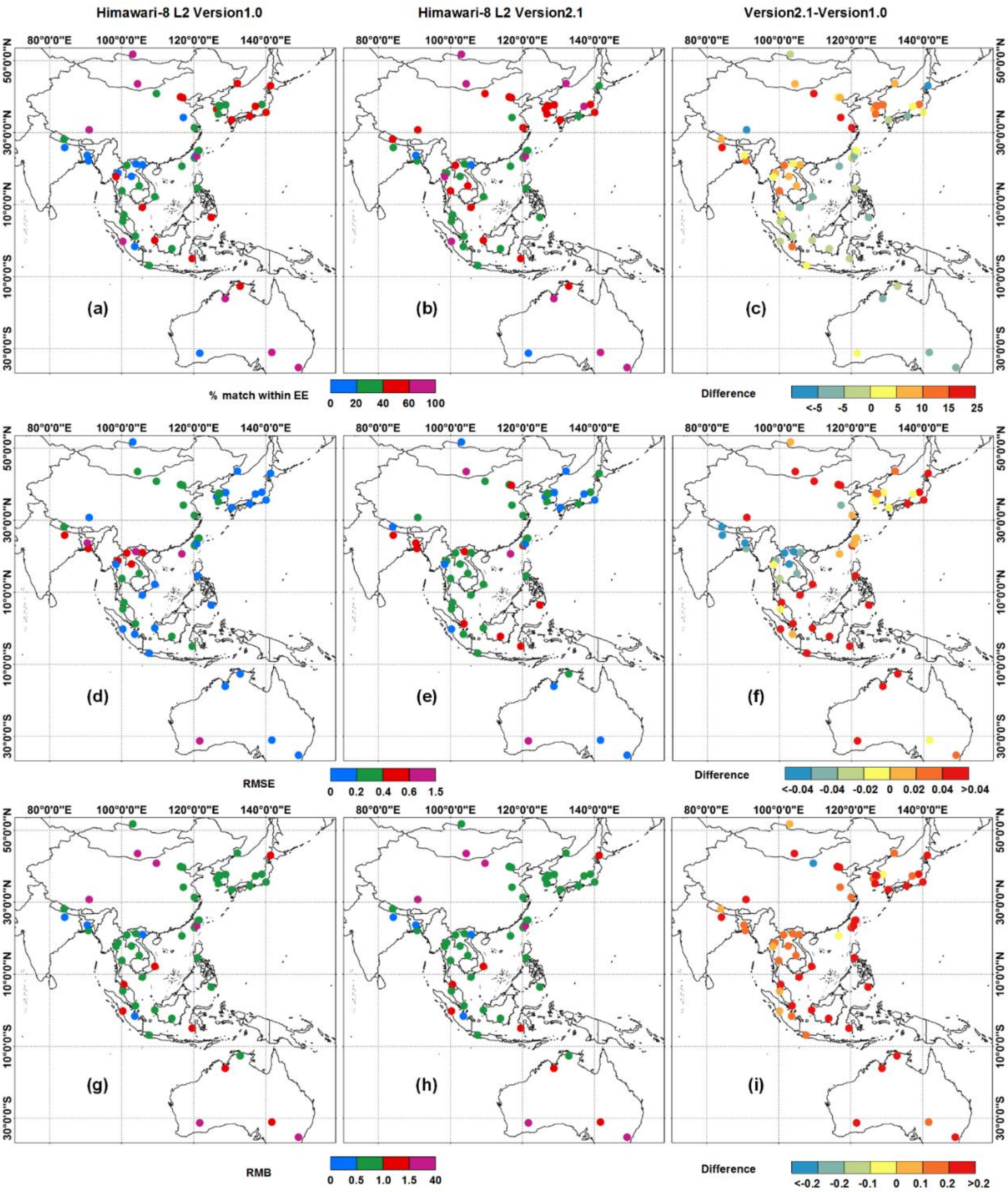

Fig. 6. Validation statistics for Himawari-8 L2 V1.0 and V2.1 AOD at 500 nm. For each site, (a,b) are the fraction of matches within the EE of AERONET, (d, e) show the root mean squared error (RMSE), and (g, h) show the relative mean bias (RMB). (c), (f), and (i) are the differences between the Himawari-8 L2 V1.0 and V2.1 AOD products represented as the fraction of matches within the EE, RMSE, and RMB, respectively.

From Fig. 1 and 6 we can see the V2.1 AOD retrievals outperformed in term of retrievals falling within the EE, but with comparatively higher RMSE compared to that of V1.0. The high RMSE of V2.1 AOD products can be found in Indo-Gangetic

Plain, Mongolian Plateau, and Southeast Asia. Moreover, The V2.1 AOD retrievals tended to overestimate the AOD at some sites of these region (Fig. 6(h)). Therefore, to explore the potential reasons for this high uncertainty of V2.1 AOD, we selected the Gandhi College (Cropland) and Dalanzadgad (Urban) sites that are located the Indo-Gangetic Plain and the Mongolian Plateau, respectively, to analyze their AOD retrievals. Table 3 showed the error statistics for V1.0 and V2.1 AOD, we found out that the V2.1 AOD (V1.0 AOD) had 44.94% (38.20%) and 40.16% (8.20%) retrievals falling within the EE in Dalanzadgad and Gandhi College, respectively. However, the RMSE, MAE and RMB values of the V2.1 AOD at both sites were much higher than those of V1.0 AOD. We then looked at the AOD retrieval distribution on two days, 10 September 2017 and 16 April 2016, at the Dalanzadgad and Gandhi College sites (Fig. 7). At the Dalanzadgad site on September 10, 2017, the V2.1 AOD value was 2.50 (Fig. 7(b)), but the value was only 0.115 as recorded with V1.0 (Fig. 7(a)). Similarly, the V2.1 AOD was also significantly higher (1.26) (Fig. 7(d)) than the V1.0 AOD (0.28) (Fig. 7(c)) at Gandhi College. This indicated that the outliers generated by the V2.1 algorithm may be the cause of its higher RMSE, MAE, and RMB as compared to that of the V1.0 algorithm. This phenomenon was attributed to the inaccurate characterization of surface reflectance. V2.1 algorithm uses two methods to determine surface reflectance: second lowest reflectance technology and an improved Kaufman method (Yoshida et al., 2018; Fukuda et al., 2013). Thus, it is possible for the estimated surface reflectance of one pixel to differ from that of its neighbors; furthermore, the underestimation of surface reflectance may lead to an overestimation of the AOD.

Table 3. Error statistics for Himawari-8 L2 V1.0 and V2.1 AOD at Dalanzadgad and Gandhi College at 05:30 (UTC)

Site	N	RMSE		MAE		RMB		Within EE (%)	
		V1.0	V2.1	V1.0	V2.1	V1.0	V2.1	V1.0	V2.1
Dalanzadgad	89	0.22	1.13	0.16	0.72	3.18	11.57	38.20	44.94
Gandhi_College	122	0.51	0.59	0.43	0.36	0.51	1.05	8.20	40.16

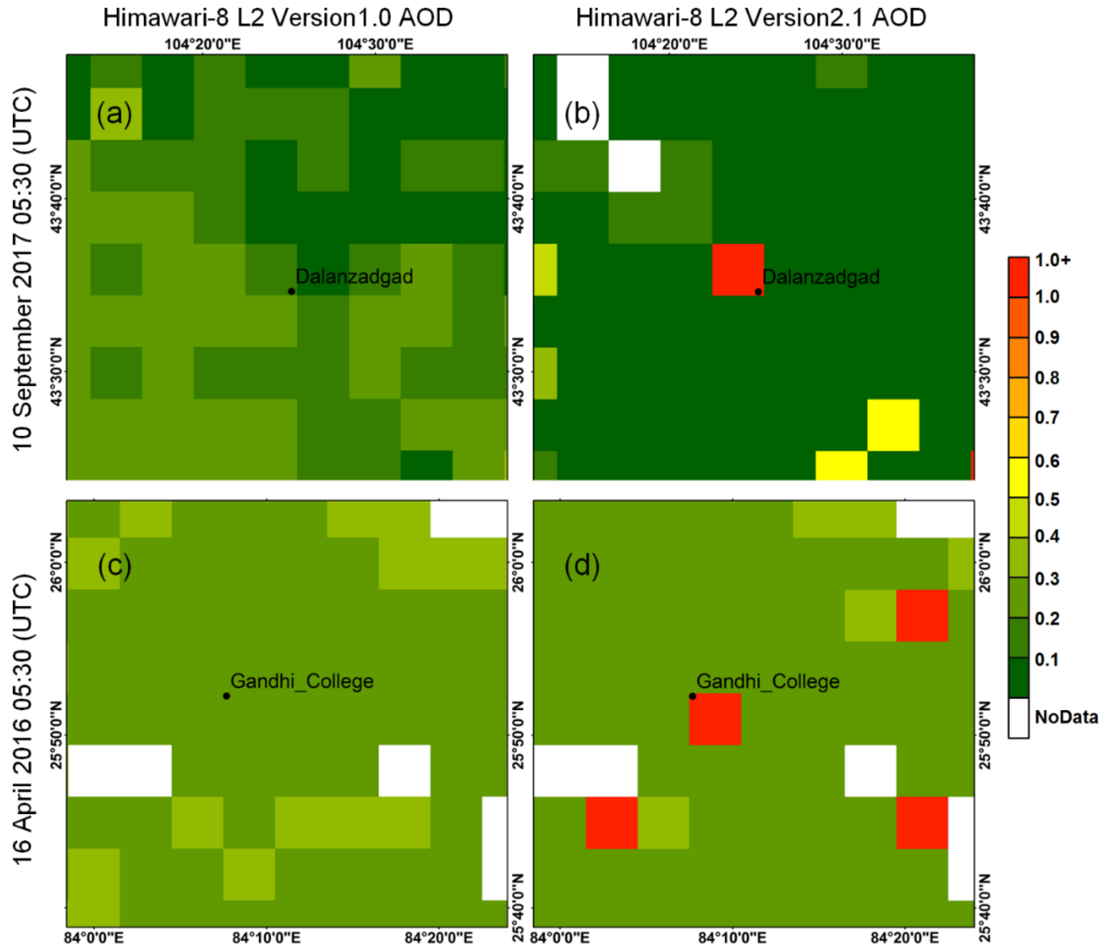

Fig. 7. Comparison of Himawari-8 L2 V1.0 ((a), (c)) and V2.1 ((b), (d)) AOD at Dalanzadgad (Mongolia) and Gandhi_College (India) on 2 days: September 10, 2017 (top row) and April 16, 2016 (bottom row). All satellite images were captured at 05:30 (UTC).

3.1.3 Spatial distributions of V1.0 and V2.1 AOD products

To compare the spatial variations of the Himawari-8 L2 V1.0 and V2.1 AOD products from 2016 to 2017, the annual mean AOD values during 00:00 to 09:50(UTC) of V1.0 (Fig. 8(a) and (d)) and V2.1 (Fig. 8(b) and (e)) were generated. It was clearly observed that the V1.0 and V2.1 AOD retrievals generally exhibited highly similar spatial patterns in aerosol loading but differed in their details. High aerosol loadings (AOD > 0.5) were mainly found in East China, West China, and the Indo-Gangetic Plain, while low aerosol loadings (AOD < 0.2) were observed in Southwest China, Japan, Sri Lanka, and Australia for both V1.0 and V2.1 AOD. From Fig.8 (c) and (f), we can see large spatial differences (> 0.2) existed between V1.0 and V2.1 algorithms in regions with high aerosol loadings (e.g., West China, the North China Plain, and the Indo-Gangetic Plain), especially in Northwestern China where the AOD differences between V1.0 and V2.1 were greater than 0.8. Meanwhile, the V2.1 AOD retrievals tended to be lower than those from V1.0 in parts of Southwestern and Northeastern China, Southwestern Russia, Japan, and Australia, where the AOD differences were observed to be between -0.2-0.

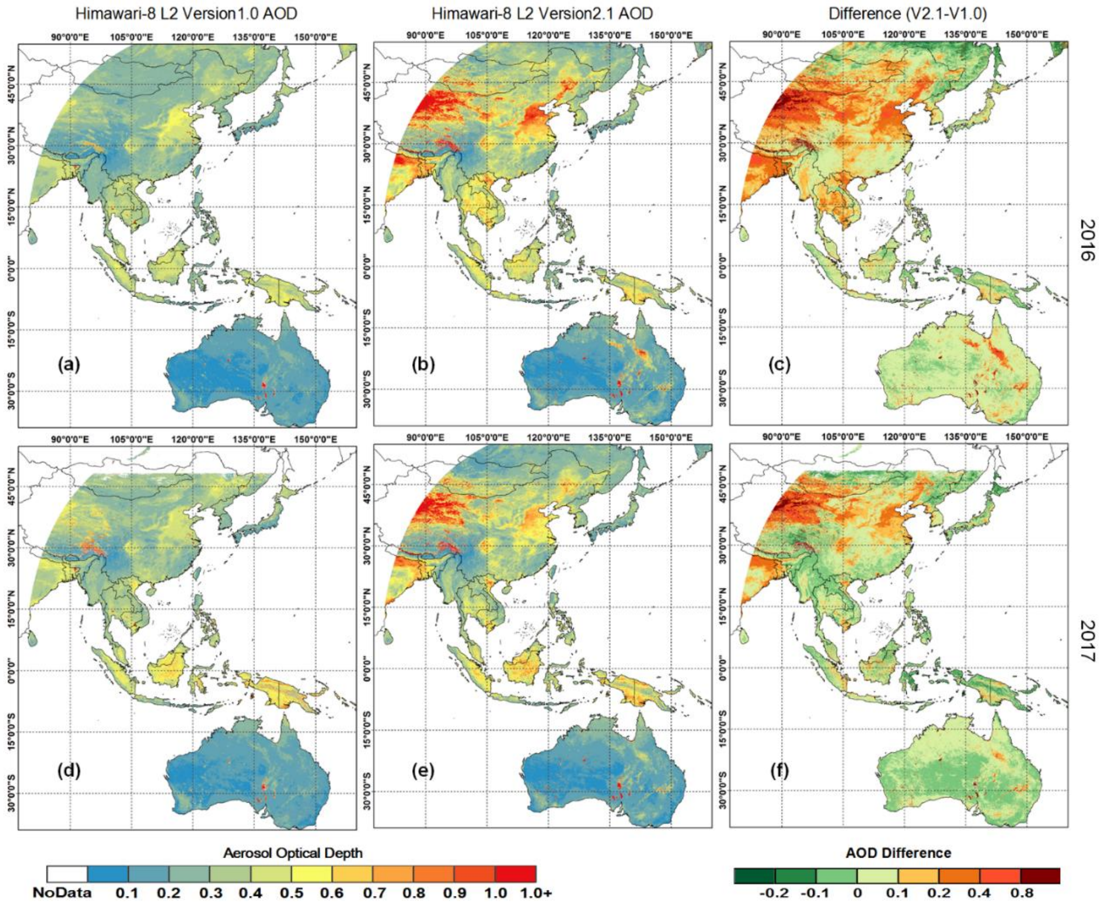

Fig. 8. Spatial distribution of the average AOD products at 500 nm from the two versions and the difference between them over the study area in 2016 and 2017.

3.1.4 Uncertainty analysis on V1.0 and V2.1 AOD products

Surface types and Surface reflectance are known to affect the accuracy of aerosol retrievals. High Normalized Difference Vegetation Index (NDVI) values indicated complete or nearly complete coverage by green vegetation, while low values indicated sparse vegetation (Burgan & Hartford, 1993). As demonstrated in Fig. 9 (a), for NDVI<0.2, the V2.1 retrievals showed positive mean biases greater than 0.17, while the V1.0 retrievals had smaller mean biases around 0.04. For 0.2 ≤NDVI ≤0.8, the V1.0 mean biases became increasingly negative (changing from -0.09 to −0.21) while the V2.1 mean biases were more stable and remains comparatively closer to zero. For the NDVI ≥0.8, both the V1.0 and V2.1 biases were close to zero, around 0.01 for V1.0 and 0.03 for V2.1. To further explore the performance of Himawari-8 L2 AOD algorithms over multifarious surfaces, we classified the data of the L2 AOD retrievals from 2016 to 2017 into five typical land cover types (i.e., forest (4 sites), cropland (6 sites), grassland (17 sites), bare land (2 sites), and urban (29 sites)) as determined by MOD12Q1 land cover data (Fig. S1). Of the three vegetation types, both V1.0 and V2.1 algorithm performed the best over forested area with the biases closer to zero (Fig. 9(b)).

Compared to the V1.0 algorithm, the performance of V2.1 algorithm was improved over the three vegetation types. However, it still showed negative biases. Meanwhile, V1.0 and V2.1 algorithm performed poorly over urban and barren land. The mean biases were negative (<-0.1) for the urban and positive (>0.14) for barren land. These results showed that the performance of V2.1 retrievals improved as compared to the V1.0 retrievals because it had more stable biases that were closer to zero.

Elevation is an important property of the underlying surface and it varies greatly among the 58 AERONET sites (Fig. S2). Therefore, we evaluated the Himawari-8 L2 AOD retrievals performance at different elevations (Fig. 9(c)). When the elevation was below 100 m, V1.0 AOD retrievals showed large negative biases around -0.15, while V2.1 AOD retrievals had smaller biases closer to zero, which indicated that V2.1 AOD retrievals performed better in low-elevation areas. For elevation in the 100-1000 m range, although the V2.1 algorithm seemingly performed better as compared to the V1.0 algorithm, both of them showed negative biases, which suggested an underestimation in the AOD. This could be due to the high frequency of human activities and a more complicated landscape in this elevation range, leading to errors in the estimation of surface reflectance and posing a challenge in satellite retrieval of aerosol properties. For high-elevation areas (height>1000 m), all two datasets showed good performances with small biases (~0) because high elevation areas tend to be sparsely populated mountains, where aerosol properties are relatively simple.

Fig. 9(d) summarized the seasonal variation of retrieval accuracy for V1.0 and V2.1 AOD, which indicated both the V1.0 and V2.1 algorithm performed the best in summer, followed by fall and winter, and the worst in spring. Similar seasonal variations in Himawari-8 AOD product biases have also occurred in China (Zhang et al., 2019). Moreover, the V1.0 algorithm tended to underestimate the AOD in every season with the mean biases being less than -0.3. As compared to V1.0 retrievals, V2.1 retrievals had smaller biases that were closer to zero.

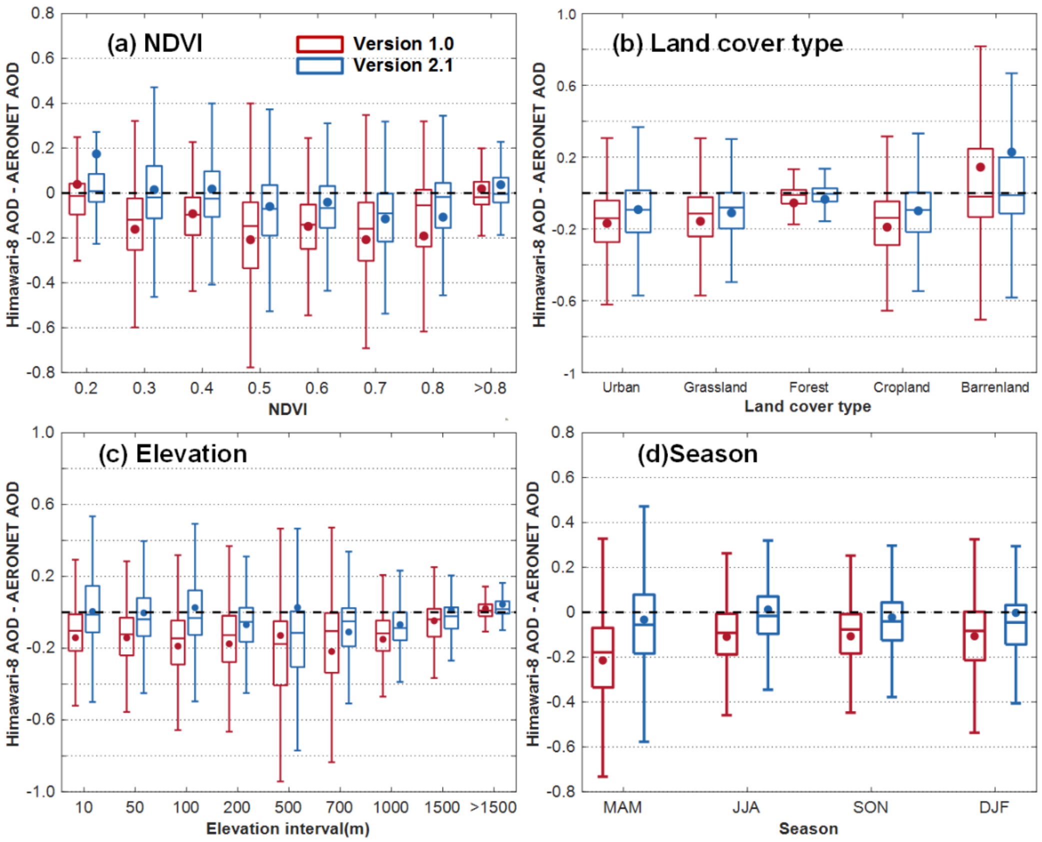

Fig. 9. Box plots of AOD errors (satellite – AERONET) relative to AERONET at 500 nm over the study area. For each box-whisker plot, the properties are as follows: height is the interquartile range of the AOD error; the middle line is the median AOD error, and the dot is the mean AOD error.

3.2 Evaluation of Himawari-8 L2 AE and FMF accuracy against AERONET

The AE is commonly used to describe the wavelength dependence of the AOD and is an important optical parameter for qualitatively measuring aerosol particle sizes. Particle size helps to distinguish and characterize different aerosol types (Kaskaoutis et al., 2006). To evaluate the accuracy of Himawari-8 AE products, we used a total of 76,362 pairs of Himawari-8 and AERONET AE data obtained from 2016 to 2017. The results indicated that the V2.1 algorithm provided more accurate AE retrievals than the V1.0 algorithm, with the fraction of AE retrievals falling within the EE being 34.64% (Fig. 10b) and 13.43% (Fig. 10a), respectively. The RMSE (0.65) and MAE (0.52) values of the V2.1 AE were significantly lower than those of the V1.0 AE (RMSE: 1.03, MAE: 0.91). Overall, although the Himawari-8 L2 AE products still demonstrated large retrieval error, their accuracy appeared to have been significantly improved with the algorithm upgrade. In Fig.10(c) and 10(d), we can see that both Himawari-8 L2 V1.0 and V2.1 Angstrom exponents are overestimated at low AE and underestimated at high AE. As compared with V1.0, V2.1 AE had smaller standard deviations at most bins. This suggested that Himawari-8 L2 V2.1 AE had a better performance than that of V1.0.

The FMF was another important physical property used to distinguish between natural and anthropogenic aerosols (Yan, Li, et al., 2017). Therefore, we evaluated the performance of the Himawari-8 L2 FMF retrievals (Fig. S3). It is evident that the retrieval accuracy of V2.1 FMF was comparatively better (within EE: 39.07%) than that of the V1.0 (within EE: 28.35 %) with lower RMSE (V1: 0.41, V2: 0.30) and MAE (V1: 0.34, V2: 0.25) (Fig. S3 (a), (b)). Similar to Himawari-8 L2 AE products, both Himawari-8 L2 V1.0 and V2.1 FMF were overestimated at low FMF and underestimated at high FMF (Fig. S3(c), (d)). Overall, both Himawari-8 FMF products showed significant underestimation, demonstrating the need for further algorithm optimization.

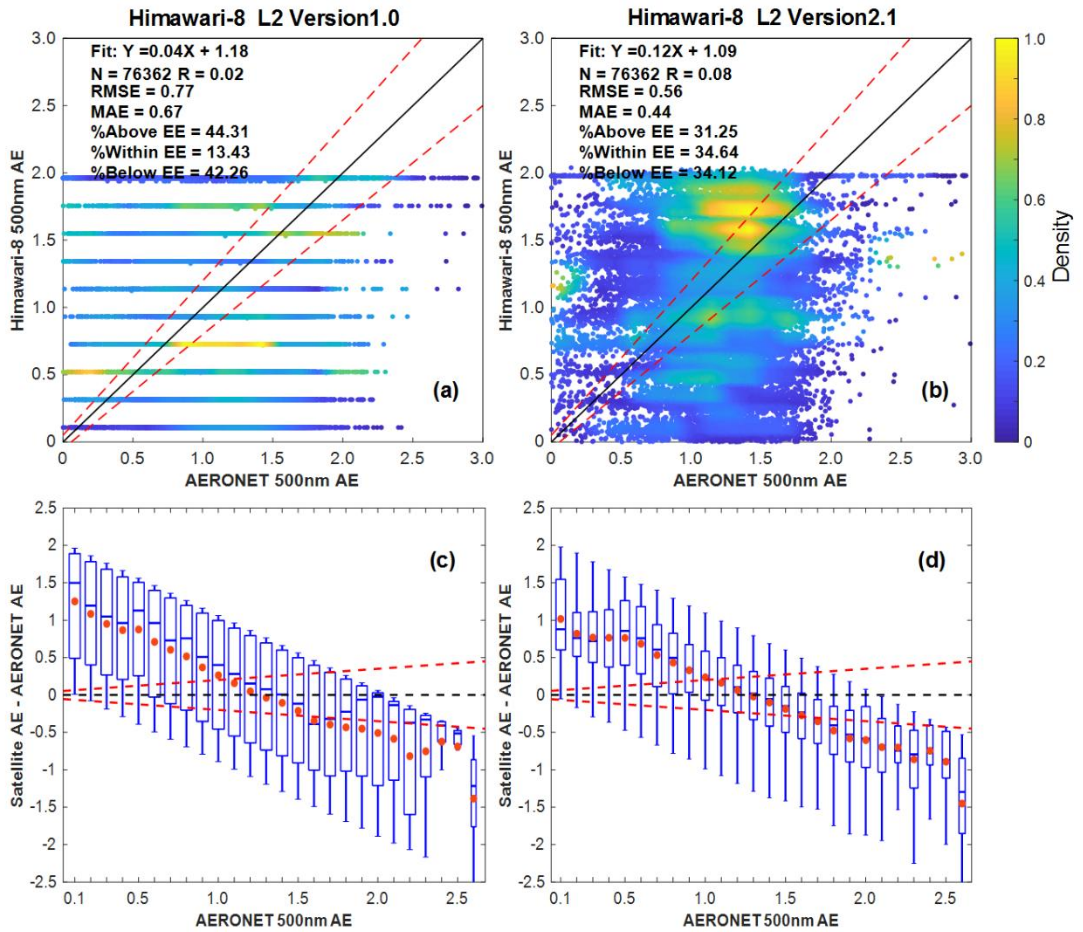

Fig. 10. Scatter plot comparing AERONET and Himawari-8 L2 V1.0 (a) and V2.1 (b) Angstrom exponent (AE) values at 500 nm from 2016 to 2017. Linear regression is shown as a solid red line. The dashed lines are the envelopes of the expected error, and the black solid line is the 1:1 line. Box plots of Himawari-8 L2 V1.0 (c) and V2.1 AE (d) errors (satellite - AERONET) at 500 nm versus AERONET AE. Data are sorted by AERONET AE at 0.1 intervals of AE. The one-one line (zero error) is shown as a black dashed line and the envelopes of the expected error are shown as red dashed lines. For each box-whisker plot, the width is the standard deviation (α) of the satellite AE; height is the interquartile range of the AE error; the middle line and the red dot are the median and mean AE error, respectively.

3.3 Comparison between Himawari-8 and MODIS AOD products

3.3.1 Accuracy of Himawari-8 and MODIS AOD products

To perform inter-comparison of retrieval accuracy and spatial variation between Himawari-8 AOD (QA=Very good) and MODIS AOD (DB:QA≥2; DT:QA=3) products in Asia, Himawari-8 L2 V2.1 AOD according to MODIS overpass time for each of 38 AERONET sites in Asia (Fig. S4) was used. Table S3 presents the UTC time of MODIS overpass time (02:30 for Terra, and 05:30 for Aqua at Local standard time (LST)) for each AERONET site. The accuracy comparison between Himawari-8 (02:30 LST) and Terra MODIS AOD products is shown in Fig.10. The number of collocation vary with the Himawari-8 L2 V2.1 AOD having the highest collocation (N: 3202) (Fig. 11(a)) followed by Terra DB (N: 1634) (Fig. 11(b)) and DT (N: 1167) (Fig. 10(c)). The DT 3 km has the lowest number of retrievals (919) (Fig. 11(d)), most likely due to its inability to retrieve AOD over sparsely vegetated, dry and bright surfaces characterized by very high surface reflectance (Levy et al., 2010). The Himawari-8 L2 V2.1 retrievals at 02:30 (LST) agree well with AERONET AOD ($R = 0.73$) with 48.63% of observations falling within the EE, and its RMSE, MAE and RMB values were 0.29, 0.16 and 0.15, respectively. By contrast, the Terra MODIS retrievals provide better agreement with AERONET AOD (R: 0.84-0.88) with more retrievals falling within the EE (DT 10 km: 57.93%, DT 3 km: 56.37%, DB: 54.59%). Furthermore, the Terra MODIS retrievals have smaller RMSE (0.19-0.22) and MAE (0.13-0.14), but slightly larger RMB (1.16-1.37) than that of retrievals from Himawari-8 L2 V2.1.

The comparison results of the Himawari-8 L2 V2.1 (05:30 LST) and Aqua MODIS AOD are shown in Fig.12. Similar to the results at 02:30, Himawari-8 had the highest number of AOD retrievals (3012) (Fig. 12(a)), followed by the DB (1634) (Fig. 11(b)), DT 10 km (990) (Fig. 12(c)), and DT 3 km (845) (Fig. 12(d)) at 05:30. V2.1 AOD at 05:30 showed a poor performance with 46.35% of retrievals falling within the EE and larger RMSE (0.37), MAE (0.19), and RMB (1.47) as compared to that with V2.1 AOD at 02:30, indicating that V2.1 retrievals at 02:30 had a better performance. The accuracy of the Aqua MODIS AOD was still higher than that of the Himawari-8 L2 V2.1 AOD. For Aqua MODIS AOD, the DT 10 km retrievals showed relatively better performance among the three datasets with 58.28% of retrievals falling within the EE, larger R (0.88), smaller RMSE (0.18), MAE (0.12), and RMB (1.13). Our findings are little different with previous verification results of MODIS

AOD (Nichol et al. 2016). For example, Nichol et al. (2016) validated the MODIS Collection6 AOD products (MYD04_3K and MYD04_L2) over Asian countries and found 55% and 63% of the retrievals for MYD04_3K and MYD04_L2 within the expected error, respectively. The main reason may be the use of MODIS AOD data for different time periods, and different AERONET sites for verification. Overall, these results indicated that the retrieval quality of the MODIS C6.1 AOD products was still better than the Himawari-8 L2 V2.1 AOD products in Asia.

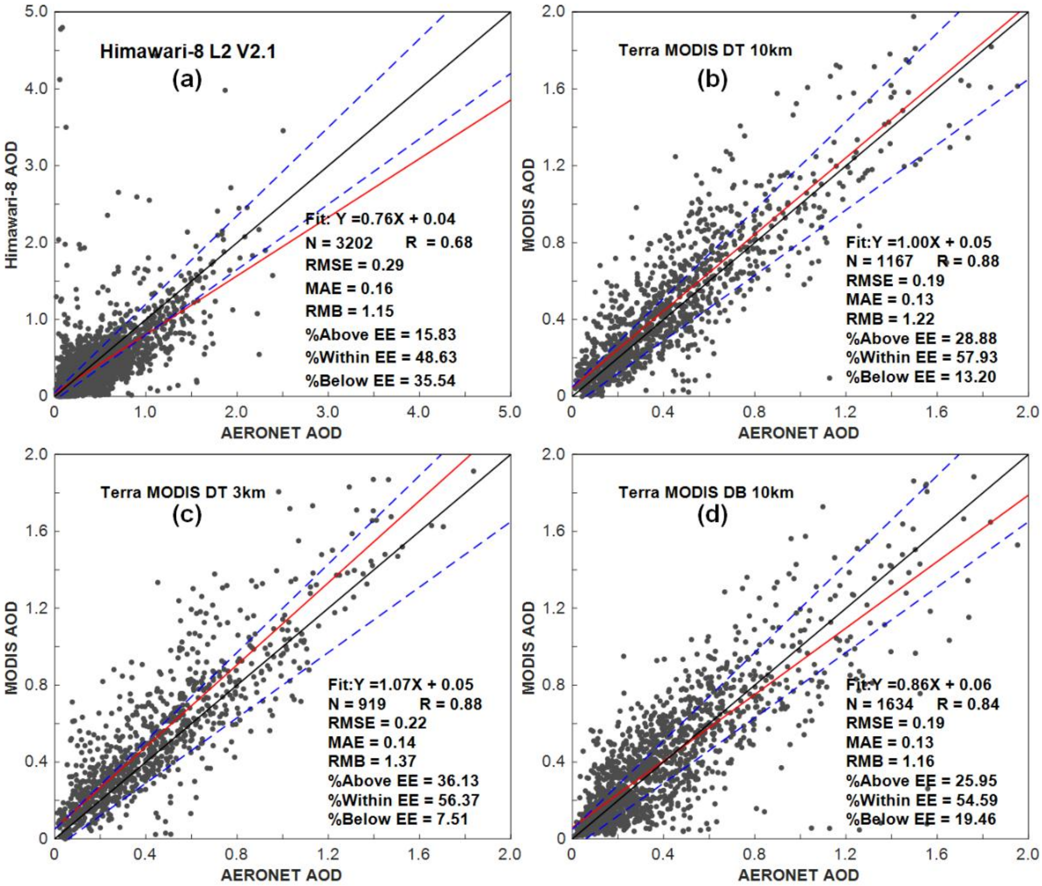

Fig. 11. Himawari-8 V2.1 AOD (02:30, LST for each site) (a) at 500nm and Terra MODIS C6.1 DT 10 km (b), DT 3 km (c), and DB 10 km (d) at 550 nm against AERONET AOD product over Asia from 2016 to 2017. The blue dashed lines are the envelopes of the expected error, the black solid line is the 1:1 line, and linear regression is shown as a solid red line.

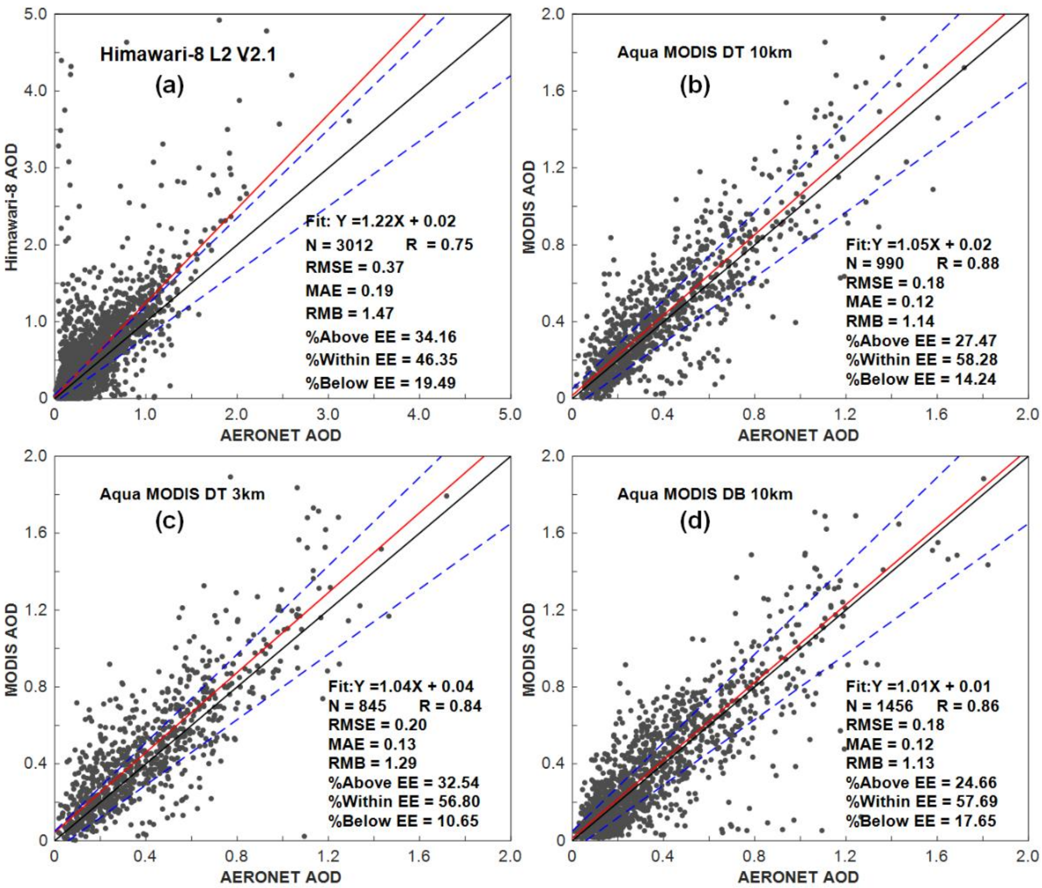

Fig. 12. Himawari-8 V2.1 AOD (05:30, LST for each site) (a) at 500 nm and Aqua MODIS C6.1 DT 10 km (b), DT 3 km (c), and DB 10 km (d) at 550 nm against AERONET AOD over Asia in the period between 2016 and 2017. The blue dashed lines are the envelopes of the expected error, the black solid line is the 1:1 line, and linear regression is shown as a solid red line.

3.3.2 Spatial variations of Himawari-8 and MODIS AOD products

Fig.13 and Fig.14 show the two-year average Himawari-8 and Terra/Aqua MODIS AOD during the four seasons in Asia, respectively. The Himawari-8 V2 algorithm provided the best coverage, with almost no missing data over the study domain, while the MODIS DT algorithm showed the lowest coverage in regions with high surface reflectance (e.g., Northwestern China), where the predominant land cover type is bare soil. From Fig. 13 and 14, we can see the Himawari-8 L2 V2.1 and Terra/Aqua MODIS C6.1 AOD showed similar spatial patterns in aerosol loading but differed in their details. Regions with similarly high aerosol loadings (AOD>0.5) were mainly those with severe air pollution, such as parts of China (Northeast Plain, North China Plain, Sichuan Basin) and the Indo-Gangetic Plain(Yan et al., 2017; Yang et al., 2018). Meanwhile, low aerosol loadings (AOD < 0.3) are found in southern parts of the Japanese and Korean peninsula, the Yunnan-Guizhou Plateau, Sri Lanka, and the Western Sichuan Plateau of China. Observations at the AERONET sites were basically consistent with the overall distribution of Himawari-8 and MODIS AOD (Fig. 15).

However, comparison of Himawari-8 and MODIS AOD products indicated that Himawari-8 overestimated AOD in regions with high aerosol loadings, especially in West China, where Himawari-8 had significantly higher AOD retrievals (AOD > 1) than MODIS (AOD < 0.7). Zhang et al. (2019) also found that the Himawari overestimated the AOD in North China Plain and West China. This result suggests that the Himawari-8 has a large bias in heavily polluted regions, which mainly results from improper estimation of surface reflectance and aerosol model. Moreover, Himawari-8 also overestimated AOD in Southeast Asia (such as Sumatra, Kalimantan and New Guinea), with an AOD range of 0.5–1.2, which is much higher than those of AERONET (0.19–0.57) and MODIS (0.01–0.4). The Himawari-8 and MODIS AOD products also showed similar seasonal spatial distribution but differed in their details. In spring and summer, large difference could be found in West China, the Indo-Gangetic Plain, and Southeast Asia. The difference between Himawari-8 and MODIS AOD can even exceed 0.6 in West China. In fall, the difference between Himawari-8 and MODIS AOD was relatively small, and both of them could reflect the AOD in East Asia and South Asia. However, the AOD of V2.1 AOD in Southeast Asia was slightly higher than that of MODIS AOD. In winter, most of the V2.1 AOD values were above the values of the MODIS AOD retrievals in West China and Southeast Asia.

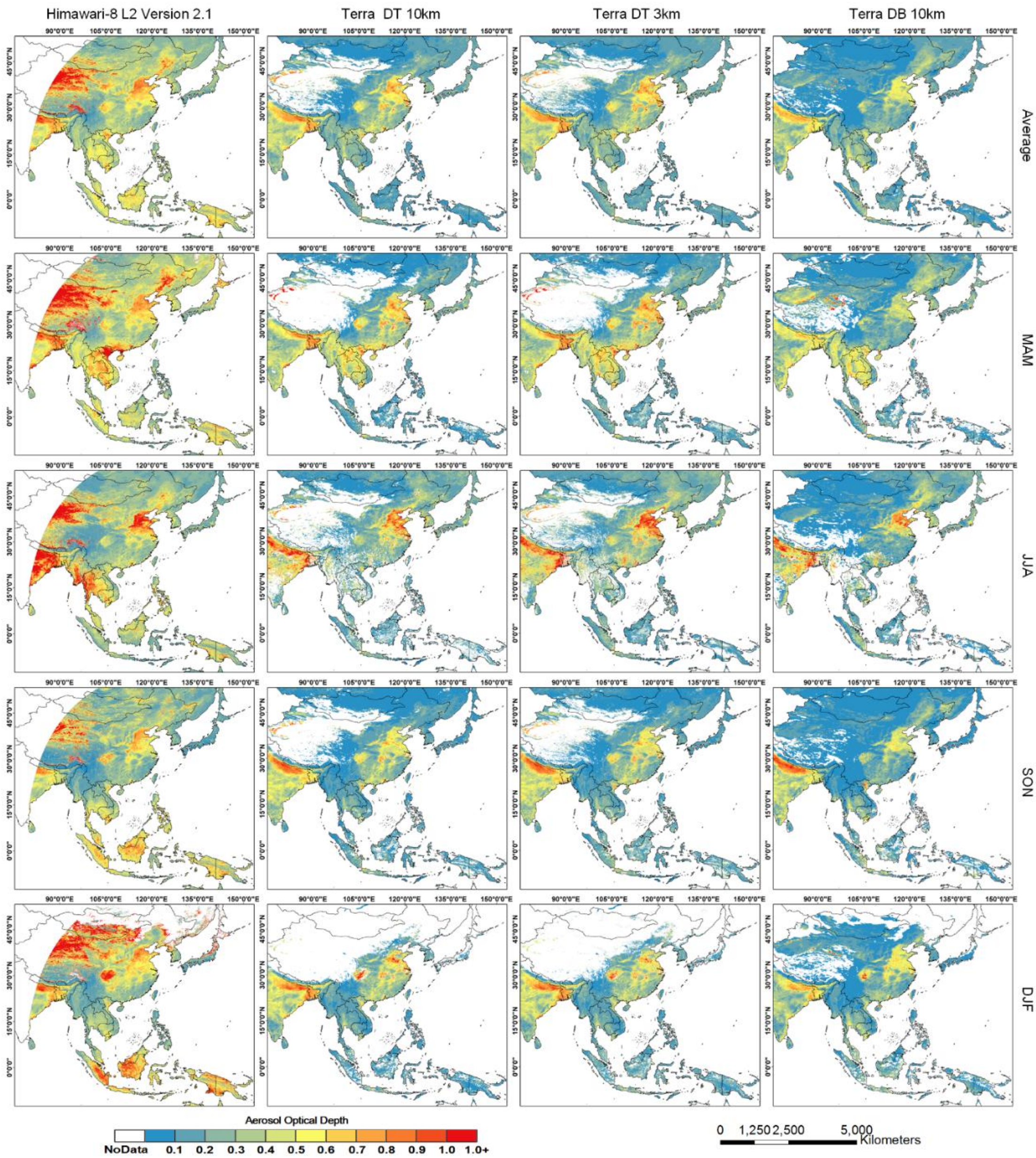

Fig. 13. Spatial distribution of the 2-year (2016-2017) average AOD over Asia using Himawari-8 L2 V2.1 (500 nm), Terra MODIS DT 10 km, DT 3 km, and DB 10 km (550 nm). "MAM," "JJA," "SON" and "DJF" are spring, summer, fall, and winter, respectively, in the northern hemisphere.

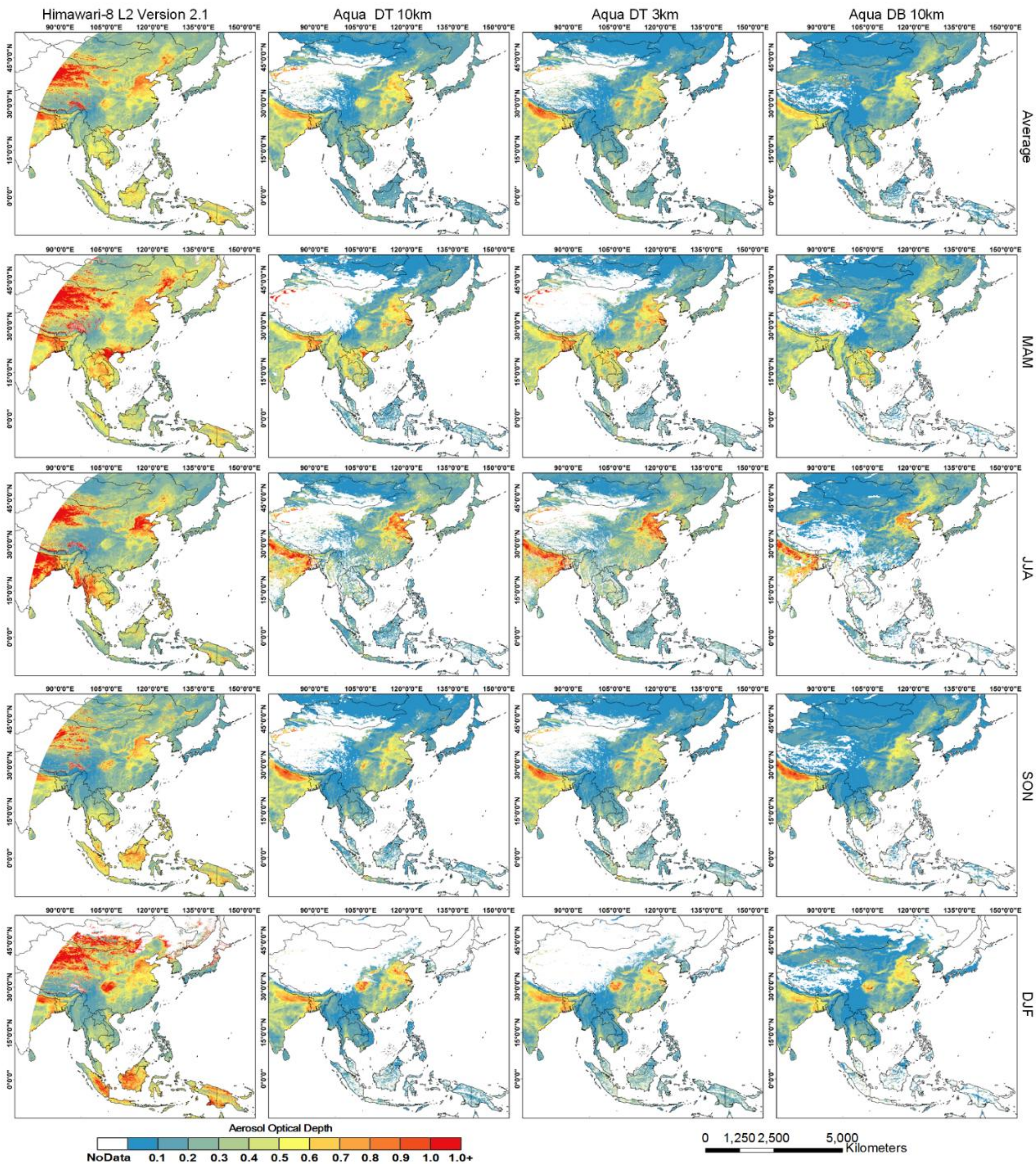

Fig. 14. Spatial distribution of the 2-year (2016-2017) average AOD over Asia for Himawari-8 L2 V2.1 (500 nm), Aqua MODIS DT 10 km, DT 3 km, and DB 10 km (550 nm). "MAM," "JJA," "SON" and "DJF" are spring, summer, fall, and winter, respectively, in the northern hemisphere.

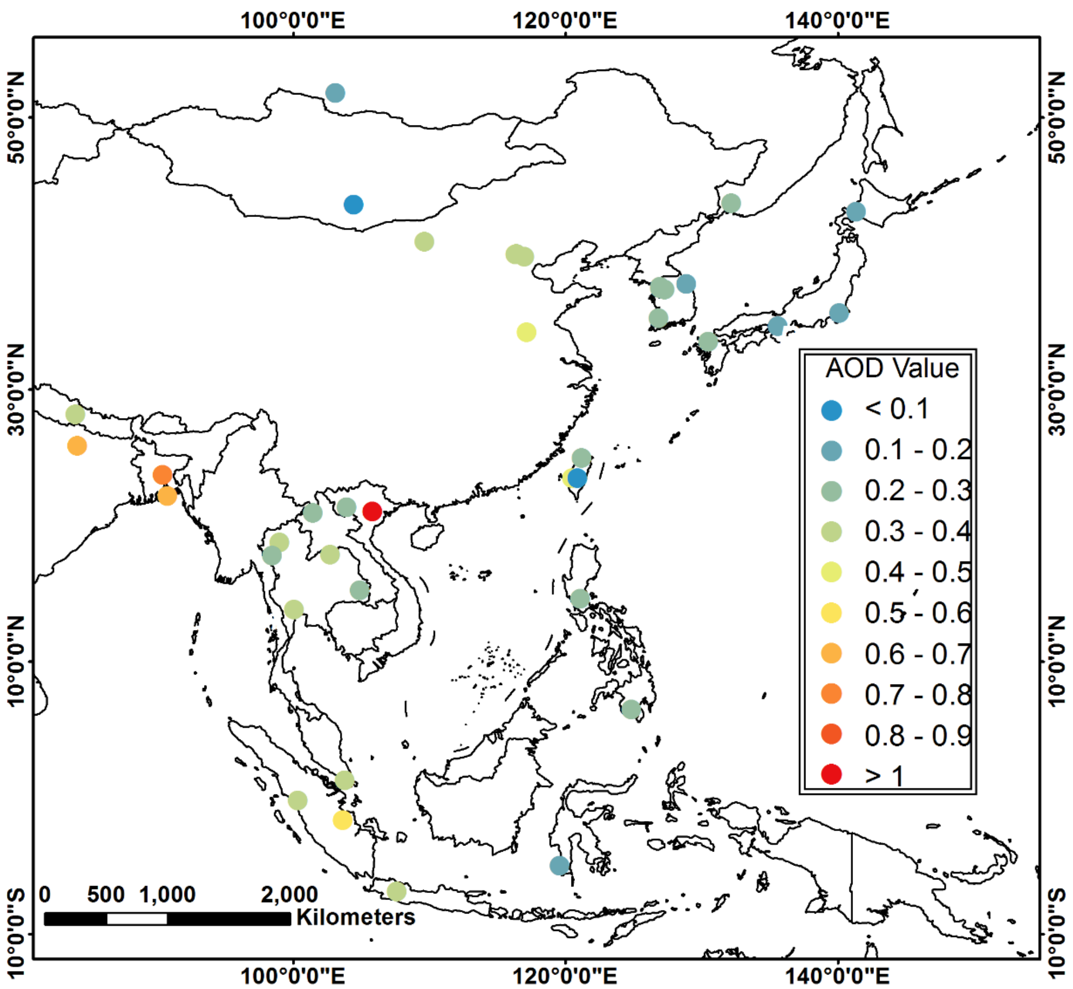

Fig. 15. The average AERONET AOD across two years (2016–2017) over Asia at each site

4. Discussion

This study compared the performance of the Himawari-8 L2 V1.0 and V2.1 aerosol products in terms of AOD retrievals. Results indicated that both V1.0 and V2.1 AOD show a high consistency with AERONET AOD (R: 0.67-0.72). V2.1 AOD has more retrievals falling within the EE but with higher RMSE and MAE than those of V1.0. The bias between Himawari-8 L2 AOD and AERONET AOD increased with the AOD magnitude, indicating that aerosol retrievals face great challenges under the condition of high AOD. On the other hand, V1.0 AOD tended to underestimate AOD, especially at high AOD values, while V2.1 AOD had a smaller mean bias and showed about zero mean bias at most AOD values. Zhang et al. (2019) also found that the bias of Himawari-8 L2 V2.0 AOD was positive when AOD lower than 0.5 and decreased with the AOD magnitude. Moreover, V2.1 AOD retrievals can more accurately reflect the daily variations and sub-hourly variations compared to that of V1.0 AOD retrievals. Site-scale evaluation and spatial distribution results showed that Himawari-8 L2 AOD overestimated AOD in Australia and Northwest China and underestimated AOD in Southeast Asia.

The uncertainty of V1.0 and V2.1 AOD varies widely with the change in the diverse land cover types, DEM, and seasons. Results showed that both V1.0 and V2.1 AOD retrievals perform much better over forested and grassland areas than over urban areas, croplands, and barren lands. Seasonal changes also affect the accuracy of aerosol retrieval. Best performance can be observed in summer, followed by fall and winter, and the worst is observed in spring. Both of the two versions of AOD products perform much better in high-elevation areas due to artifact reduction, while they perform poorly at elevations of 100-1000 m.

Results indicate that the total underestimation of the V2.1 AOD was improved and more retrievals falling within the EE compared to the V1.0 AOD (Fig.2). Li et al. (2019) found similar results by validating Himawari-8 L2 (V1.0 and V2.0) and L3 AOD products in Eastern China. The Himawari-8 L2 V1.0 AOD retrieval interval was 0.0-2.0, which may have led to an underestimation of the AOD values in areas, where the aerosol loadings were extremely high (Daisaku, 2016). However, V2.1 AOD still have large estimation uncertainties in high aerosol loadings areas and sparsely vegetated areas. For example, this study demonstrates that V2.1 algorithm tends to overestimate the AOD in Northwest China. Overall, the identified large biases of highly polluted area and sparsely vegetated areas in V2.1 AOD product may be due to the inaccurate characterization of surface reflectance and aerosol model (Zhang et al., 2019).

5. Conclusions

In this study, we evaluated the performance of aerosol products (AOD, AE, and FMF) of the two versions (V1.0 and V2.1) of Himawari-8 against 58 AERONET observations and analyzed the uncertainty in Himawari-8 L2 AOD products. Furthermore, we compared the Himawari-8 L2 V2.1 and MODIS C6.1 AOD products in terms of accuracy and spatial variations.

Our main conclusions are as follows. Both V1.0 and V2.1 AOD showed a high consistency with AERONET AOD (R: 0.67-0.72) with 44.65% and 49.38% of retrievals fell within the EE, respectively. Both of the V1.0 and V2.1 AOD bias increased with the AOD magnitude, but V1.0 AOD tended to underestimate the AOD, especially at high AOD values. The underestimation has now improved in the V2.1 AOD products. Moreover, V2.1 AOD retrievals can more accurately capture daily variations and sub-hourly variations compared to the V1.0 AOD. The uncertainty analysis showed that the V1.0 and V2.1 algorithm performed worse over sparsely vegetated surfaces (low NDVI) but improved as NDVI increased. Both V1.0 and V2.1 AOD performed better over forests and grasslands than croplands, as well as urban and barren lands. Meanwhile, V1.0 and V2.1 AOD had the best performance in summer, while the worst in spring and performed better in high-elevation areas. Overall, the V2.1 AOD outperformed in term of retrievals falling within the EE compared to V1.0 AOD, but V2.1 AOD still have large estimation uncertainties in high aerosol loadings areas and sparsely vegetated areas.

We also compared the Himawari-8 AE and FMF retrievals (AOD size parameters) with those of AERONET. The results showed that the accuracy of V2.1 AE/FMF products was significantly higher than that of V1.0, with more retrievals falling within the EE with lower RMSE and MAE values. However, the Himawari-8 V2.1 AE and FMF products still exhibited large estimation error on all scales, showing overestimations at low values and underestimations at high values.

With the comparison between Himawari-8 and MODIS AOD products, we found that the V2.1 AOD obtained more retrievals due to the high revisit frequency, but the MODIS AOD provided a better agreement (R: 0.84-0.88) with more retrievals falling within the EE (Terra: 57.93% (DT 10 km), 56.37% (DT 3 km), 54.49% (DB); Aqua: 58.28% (DT 10 km), 56.80% (DT 3 km), 57.69% (DB), as well as lower RMSE (0.18-0.22), MAE(0.12-0.16), and RMB (1.13-1.37) compared to that of V2.1 AOD. Furthermore, the V2.1 and Terra/Aqua MODIS C6.1 AOD showed relatively similar spatial patterns in aerosol loading, but V2.1 AOD tended to be overestimated in northwestern China and Southeast Asia. Although the accuracy of Himawari-8 L2 V2.1 AOD products were recorded to be slightly lower than MODIS C6.1 AOD products, it can still provide real-time monitoring aerosol properties over Asia and Oceania regions, which can be used to capture dynamic aerosol variations. Furthermore, Himawari-8 L2 V2.1 AOD products could help fill the data gaps in existing satellite data.

Acknowledgements

This work was supported by the National Key Research and Development Plan of China (2017YFC1501702), the National Natural Science Foundation of China (91544217, 41801329 and 91837204), and the Fundamental Research Funds for the Central Universities. The authors gratefully acknowledge the MODIS and AERONET teams for their effort in making the data available. We would like to thank the Meteorological Satellite Center (MSC) of the Japan Meteorological Agency (JMA) for providing Himawari-8 data.

References

Bilal, M.; Nichol, J.; Wang, L. New customized methods for improvement of the MODIS c6 dark target and deep blue merged aerosol product. *Remote Sensing of Environment*.2017,197, 115-124.

Bessho, K., Date, K., Hayashi, M., Ikeda, A., Imai, T., Inoue, H., . . . Yoshida, R. (2016). An Introduction to Himawari-8/9— Japan’s New-Generation Geostationary Meteorological Satellites. *Journal of the Meteorological Society of Japan. Ser. II, 94*(2), 151-183. doi:10.2151/jmsj.2016-009

Burgan, R. E., & Hartford, R. A. (1993). Monitoring vegetation greenness with satellite data.

Butt, E. W., Rap, A., Schmidt, A., Scott, C. E., Pringle, K. J., Reddington, C. L., . . . Yang, H. (2016). The impact of residential combustion emissions on atmospheric aerosol, human health and climate. *Atmospheric Chemistry & Physics, 15*(14), 20449–20520.

Chu, D. A., Kaufman, Y. J., Ichoku, C., Remer, L. A., Tanré, D., & Holben, B. N. (2002). Validation of MODIS aerosol optical depth retrieval over land. *Geophysical Research Letters, 29*(12), MOD2-1-MOD2-4. doi:10.1029/2001gl013205

Chu, D. A., Kaufman, Y. J., Zibordi, G., Chern, J. D., Mao, J., Li, C. C., & Holben, B. N. (2003). Global monitoring of air pollution over land from the Earth Observing System-Terra Moderate Resolution Imaging Spectroradiometer (MODIS). *Journal of Geophysical Research, 108*(D21), -.

Cox, C. , & Munk, W. . (1954). Measurement of the roughness of the sea surface from photographs of the suns glitter. Journal of the Optical Society of America, 44(11), 838-850.

Daisaku, U. (2016). Aerosol Optical Depth product derived from Himawari-8 data for Asian dust monitoring. *METEOROLOGICAL SATELLITE CENTER TECHNICAL NOTE, No.61, MARCH, 2016*.

Diner, D. J., Braswell, B. H., Davies, R., Gobron, N., Hu, J., Jin, Y., . . . Muller, J. P. (2005). The value of multiangle measurements for retrieving structurally and radiatively consistent properties of clouds, aerosols, and surfaces. *Remote Sensing of Environment, 97*(4), 495-518.

Eck, T. F., Holben, B. B. N., Reid, J. S., Dubovik, Smirnov, A., Neill, . . . Kinne, S. (1999). Wavelength dependence of the optical depth of biomass burning, urban, and desert dust aerosols. *Journal of Geophysical Research Atmospheres, 104*(D24), 31333-31349.

Emili, E., Lyapustin, A., Wang, Y., Popp, C., Korkin, S., Zebisch, M., . . . Petitta, M. (2011). High spatial resolution aerosol retrieval with MAIAC: Application to mountain regions. *Journal of Geophysical Research Atmospheres, 116*(D23), -.

Friedl, M. A., Sulla-Menashe, D., Tan, B., Schneider, A., Ramankutty, N., Sibley, A., & Huang, X. (2010). MODIS Collection 5 global land cover: Algorithm refinements and characterization of new datasets. *Remote Sensing of Environment, 114*(1), 168-182. doi:https://doi.org/10.1016/j.rse.2009.08.016

Fukuda, S., Nakajima, T., Takenaka, H., Higurashi, A., Kikuchi, N., Nakajima, T. Y., & Ishida, H. (2013). New approaches to removing cloud shadows and evaluating the 380 nm surface reflectance for improved aerosol optical thickness retrievals from the GOSAT/TANSO-Cloud and Aerosol Imager. *Journal of Geophysical Research Atmospheres, 118*(24), 13-13,531.

Gupta, P., Remer, L. A., Levy, R. C., & Mattoo, S. (2018). Validation of MODIS 3 km land aerosol optical depth from NASA's EOS Terra and Aqua missions. *Atmos. Meas. Tech., 11*(5), 3145-3159. doi:10.5194/amt-11-3145-2018

HOLBEN, B., N., ECK, T., F., SLUTSKER, TANRE, . . . J., P. (1998). AERONET : A federated instrument network and Data archive for aerosol characterization. *Remote Sensing of Environment, 66*(1), 1-16.

Hsu, N. C., Jeong, M. J., Bettenhausen, C., Sayer, A. M., & Tsay, S. C. (2013). Enhanced Deep Blue aerosol retrieval algorithm: The second generation. *Journal of Geophysical Research Atmospheres, 118*(16), 9296-9315.

Hsu, N. C., Tsay, S. C., King, M. D., & Herman, J. R. (2004). Aerosol properties over bright-reflecting source regions. *IEEE Transactions on Geoscience & Remote Sensing, 42*(3), 557-569.

IPCC. (2013). *Climate Change 2013: The Physical Science Basis. Contribution of Working Group I to the Fifth Assessment Report of the Intergovernmental Panel on Climate Change* (T. F. Stocker, D. Qin, G.-K. Plattner, M. Tignor, S. K. Allen, J. Boschung, A. Nauels, Y. Xia, V. Bex, & P. M. Midgley Eds.). Cambridge, United Kingdom and New York, NY, USA: Cambridge University Press.

Kaskaoutis, D. G., Kambezidis, H. D., Adamopoulos, A. D., & Kassomenos, P. A. (2006). On the characterization of aerosols using the Ångström exponent in the Athens area. *Journal of Atmospheric and Solar-Terrestrial Physics, 68*(18), 2147-2163.

doi:https://doi.org/10.1016/j.jastp.2006.07.008

Kaufman, Y. J., Tanré, D., Remer, L. A., Vermote, E. F., Chu, A., & Holben, B. N. (1997). Operational remote sensing of tropospheric aerosol over land from EOS moderate resolution imaging spectroradiometer. *Journal of Geophysical Research Atmospheres, 102*(27), 51-17.

Levy, H., Horowitz, L. W., Schwarzkopf, M. D., Ming, Y., Golaz, J. C., Naik, V., & Ramaswamy, V. (2013). The roles of aerosol direct and indirect effects in past and future climate. *Journal of Geophysical Research Atmospheres, 118*(10), 4521-4532.

Levy, R. C., Mattoo, S., Munchak, L. A., Remer, L. A., Sayer, A. M., Patadia, F., & Hsu, N. C. (2013). The Collection 6 MODIS aerosol products over land and ocean. *Atmos. Meas. Tech., 6*(11), 2989-3034. doi:10.5194/amt-6-2989-2013

Levy, R. C., Remer, L. A., Kleidman, R. G., Mattoo, S., Ichoku, C., Kahn, R., & Eck, T. F. (2010). Global evaluation of the Collection 5 MODIS dark-target aerosol products over land. *Atmos. Chem. Phys., 10*(21), 10399-10420. doi:10.5194/acp-10-10399-2010

Li, D., Qin, K., Wu, L., Xu, J., Letu, H., Zou, B., . . . Li, Y. (2019). Evaluation of JAXA Himawari-8-AHI Level-3 Aerosol Products over Eastern China. Atmosphere, 10(4), 215.

Li, Z., Lau, K. M., Ramanathan, V., Wu, G., Ding, Y., Manoj, M. G., . . . Zhou, T. (2016). Aerosol and Monsoon Climate Interactions over Asia: Aerosol and Monsoon Climate Interactions. *Reviews of Geophysics, 54*(1-4).

Mano, Y., Hashimoto, T., & Okuyama, A. (2009). Verification of satellite-derived aerosol optical thickness over land with AERONET data. *Papers in Meteorology and Geophysics, 60*, 7-16.

Mehta, M., Singh, R., Singh, A., Singh, N., & Anshumali. (2016). Recent global aerosol optical depth variations and trends — A comparative study using MODIS and MISR level 3 datasets. *Remote Sensing of Environment, 181*, 137-150.

Mhawish, A., Banerjee, T., Broday, D. M., Misra, A., & Tripathi, S. N. (2017). Evaluation of MODIS Collection 6 aerosol retrieval algorithms over Indo-Gangetic Plain: Implications of aerosols types and mass loading. *Remote Sensing of Environment, 201*.

Nichol, J. E., & Bilal, M. (2016). Validation of MODIS 3 km Resolution Aerosol Optical Depth Retrievals Over Asia. *Remote Sensing, 8*(4), 328.

Omar, A. H., Won, J. G., Winker, D. M., Yoon, S. C., Dubovik, O., & Mccormick, M. P. (2005). Development of global aerosol models using cluster analysis of Aerosol Robotic Network (AERONET) measurements. *Journal of Geophysical Research Atmospheres, 110*(D10), -.

Paasonen, P., Asmi, A., Petäj, Auml, T., Kajos, M. K., Ijäl, . . . Birmili, W. (2013). Warming-induced increase in aerosol number concentration likely to moderate climate change. *Nature Geoscience, 6*(6), 438-442.

Remer, L. A., Kleidman, R. G., Levy, R. C., Kaufman, Y. J., Tanré, D., & Mattoo, S. (2008). Global aerosol climatology from the MODIS satellite sensors. *Journal of Geophysical Research Atmospheres, 113*(D14), 752-752.

Saide, P. E., Kim, J., Song, C. H., Choi, M., Cheng, Y., & Carmichael, G. R. (2015). Assimilating next generation geostationary aerosol optical depth retrievals can improve air quality simulations. *Geophysical Research Letters, 41*(24), 9188-9196.

Salomonson, V. V., Barnes, W. L., Maymon, P. W., Montgomery, H. E., & Ostrow, H. (1989). MODIS: Advanced facility instrument for studies of the Earth as a system. *Geoscience &*

Remote Sensing IEEE Transactions on, 27(2), 145-153.

Sayer, A. M., Hsu, N. C., Bettenhausen, C., & Jeong, M. J. (2013). Validation and uncertainty estimates for MODIS Collection 6 “Deep Blue” aerosol data. *Journal of Geophysical Research Atmospheres, 118*(14), 7864-7872.

Sayer, A. M., Munchak, L. A., Hsu, N. C., Levy, R. C., Bettenhausen, C., & Jeong, M. J. (2015). MODIS Collection 6 aerosol products: Comparison between Aqua's e-Deep Blue, Dark Target, and ‘merged’ datasets, and usage recommendations. *Journal of Geophysical Research Atmospheres, 119*(24), 13,965-913,989.

Sayer, A. M., Smirnov, A., Hsu, N. C., & Holben, B. N. (2012). A pure marine aerosol model for use in remote sensing applications. *Journal of Geophysical Research Atmospheres, 117*(D5), -.

Sayer, A.M.; Munchak, L.A.; Hsu, N.C.; Levy, R.C.; Bettenhausen, C.; Jeong, M.J. (2014)MODIS collection 6aerosol products: Comparison between aqua's e-deep blue, dark target, and "merged" data sets, and usagerecommendations. *Journal of Geophysical Research Atmospheres*. 119, 13965-13989.

Schepanski, K. (2018). Transport of Mineral Dust and Its Impact on Climate. *Geosciences, 8*(5), 151.

Sekiyama, T. T., Yumimoto, K., Tanaka, T. Y., Nagao, T., & Murakami, H. (2016). Data Assimilation of Himawari-8 Aerosol Observations: Asian Dust Forecast in June 2015. *SOLA - Scientific Online Letters on the Atmosphere, 12*, 86-90.

Wang, W., Mao, F., Du, L., Pan, Z., Gong, W., & Fang, S. (2017). Deriving Hourly PM2.5 Concentrations from Himawari-8 AODs over Beijing–Tianjin–Hebei in China. *Remote Sensing, 9*(8), 858.

Wickramasinghe, C., Jones, S., Reinke, K., & Wallace, L. (2016). Development of a Multi-Spatial Resolution Approach to the Surveillance of Active Fire Lines Using Himawari-8. *Remote Sensing, 8*(11), 932.

Xiao, Q., Zhang, H., Choi, M., Li, S., Kondragunta, S., Kim, J., . . . Liu, Y. (2015). Evaluation of VIIRS, GOCI, and MODIS Collection 6 AOD retrievals against ground sunphotometer measurements over East Asia. *Atmospheric Chemistry & Physics Discussions, 16*(3), 20709-20741.

Yan, X., Li, Z., Luo, N., Shi, W., Zhao, W., Yang, X., & Jin, J. (2018). A minimum albedo aerosol retrieval method for the new-generation geostationary meteorological satellite Himawari-8. *Atmospheric Research, 207*.

Yan, X., Li, Z., Shi, W., Luo, N., Wu, T., & Zhao, W. (2017). An improved algorithm for retrieving the fine-mode fraction of aerosol optical thickness, part 1: Algorithm development. *Remote Sensing of Environment, 192*, 87-97.

Yan, X., Shi, W., Li, Z., Li, Z., Luo, N., Zhao, W., . . . Yu, X. (2017). Satellite-based PM2.5 estimation using fine-mode aerosol optical thickness over China. *Atmospheric Environment, 170*, 290-302. doi:https://doi.org/10.1016/j.atmosenv.2017.09.023

Yang, F., Wang, Y., Tao, J., Wang, Z., Fan, M., De Leeuw, G., & Chen, L. (2018). Preliminary Investigation of a New AHI Aerosol Optical Depth (AOD) Retrieval Algorithm and Evaluation with Multiple Source AOD Measurements in China. *Remote Sensing, 10*(5), 748.

Yang, X., Jiang, L., Zhao, W., Xiong, Q., Zhao, W., & Yan, X. (2018). Comparison of

Ground-Based PM2.5 and PM10 Concentrations in China, India, and the U.S. *International Journal of Environmental Research and Public Health, 15*(7), 1382.

Yong, X., Yan, Z., Xiong, X., Qu, J. J., & Che, H. (2011). Validation of MODIS aerosol optical depth product over China using CARSNET measurements. *Atmospheric Environment, 45*(33), 5970-5978.

Yoshida, M., Kikuchi, M., Nagao, T. M., Murakami, H., Nomaki, T., & Higurashi, A. (2018). Common Retrieval of Aerosol Properties for Imaging Satellite Sensors. *Journal of the Meteorological Society of Japan. Ser. II, advpub*. doi:10.2151/jmsj.2018-039

Zang, L., Mao, F., Guo, J., Gong, W., Wang, W., & Pan, Z. (2018). Estimating hourly PM1 concentrations from Himawari-8 aerosol optical depth in China. Environmental Pollution, 241, 654-663.

Zhang, X. Y., Wang, Y. Q., Niu, T., Zhang, X. C., Gong, S. L., Zhang, Y. M., & Sun, J. Y. (2012). Atmospheric aerosol compositions in China: spatial/temporal variability, chemical signature, regional haze distribution and comparisons with global aerosols. *Atmos. Chem. Phys., 12*(2), 779-799. doi:10.5194/acp-12-779-2012

Zhang, Z., Wu, W., Fan, M., Tao, M., Wei, J., Jin, J., . . . Wang, Q. (2019). Validation of Himawari-8 aerosol optical depth retrievals over China. *Atmospheric Environment, 199*, 32-44. doi:https://doi.org/10.1016/j.atmosenv.2018.11.024